

Signed graphs in data sciences via communicability geometry

Fernando Diaz-Diaz and Ernesto Estrada

*Institute of Cross-Disciplinary Physics and Complex Systems,
IFISC (UIB-CSIC), 07122 Palma de Mallorca, Spain*

Signed graphs are an emergent way of representing data in a variety of contexts where conflicting interactions exist. These include data from biological, ecological, and social systems. Here we propose the concept of communicability geometry for signed graphs, proving that metrics in this space, such as the communicability distance and angles, are Euclidean and spherical. We then apply these metrics to solve several problems in data analysis of signed graphs in a unified way. They include the partitioning of signed graphs, dimensionality reduction, finding hierarchies of alliances in signed networks as well as the quantification of the degree of polarization between the existing factions in systems represented by this type of graphs.

1. INTRODUCTION

Data emerging from a variety of contexts can be represented in the form of signed graphs [1, 2]. A signed graph $\Sigma = (G, \sigma)$ consists of an underlying graph $G = (V, E)$ and a signature function $\sigma : E \rightarrow \{1, -1\}$ [3]. The vertices $v_i \in V$ of G are used to represent the entities of complex systems ranging from molecular and cellular to ecological and social ones [4–13]. The edges, representing the interactions between these entities, are signed according to the nature of these interactions, with positive signs reserved for activation, cooperation, friendship, alliances, etc., while the negative ones are used to represent inhibition, competition, foes, enmity, etc. For instance, in a transcription network [5], positive/negative edges represent the activation/inhibition activity of a transcription factor on a target gene, which are represented as the vertices of the graph. In chemical reaction networks, like metabolic and signalling ones [5], a signed edge may be used to represent the contribution (accelerating or slowing down) of a molecular species to a kinetic reaction. In ecological systems [6, 14], it happens that some organisms interact with others via positive links such as mutualistic and facilitation interactions, while others do so via negative links in the form of competitive and parasitic interactions, all of them occurring at the same time. The interactions between the entities of a complex system are, in many occasions, extracted from the real-world via correlations of different nature. This is the case, for instance, of financial networks [15, 16] where correlations between stocks are frequently used to represent the possible causal connections between the entities. Social systems are, by far, the richest sources of signed interactions between entities forming a network. They include the cases of friends/foes and collaborators/defectors in face-to-face networks [4], the “like/dislike” of other’s opinions in online social networks and recommendation systems of products [9], as well as systems of alliances and conflicts in anthropology [17–19], the study of elections and voting systems in different scenarios [20–23], and the evolution of international relations between countries during regional/global conflicts [11–13, 24–29].

The study of signed graphs is an active area of investigation in mathematics [3], with roots in the works of Harary in the 1950’s [30–32]. There have been many recent advances in the understanding of structural properties of signed networks as well as on dynamical processes taking place on them [5, 7, 9, 10, 13, 16, 21, 22, 26, 29, 33–39]. However, seeing these graphs as a way of representing complex data [1, 2] immediately triggers a series of research questions. For instance, (i) how can a signed graph be partitioned to detect the main factions existing in the data; (ii) considering the signed graph as an n -dimensional space of data, how can we reduce its dimensionality?; (iii) is there a hierarchy of alliances in a signed graph?; (iv) how much polarization do the existing factions have?; (v) can we predict missing signed edges from the existing data? (see the section Related work for details). One way of tackling collectively these problems is by using machine learning techniques resting on pairwise distances between data points. A distance metric defines the geometry of an underlying space, such as Euclidean, spherical or hyperbolic ones, which are at the core of many machine learning algorithms [1]. The definition of such metrics for signed graphs is the main goal of this work.

In this work we define the concept of communicability geometry for graphs with signs. Particularly, we define the communicability distance and angles for signed graphs, which is based on the matrix exponential of the signed adjacency matrix. We prove that these metrics are Euclidean and spherical, showing several interesting properties for their use in data analysis based on signed graphs. We apply the communicability metrics to solve in a unified way the problems of signed graph partition, dimensionality reduction, finding hierarchies of alliances in signed networks as well as the quantification of the degree of polarization between the existing factions in systems represented by this type of graph. Although we do not tackle the problem of predicting missing signed edges in signed graphs, the methods developed here can be applied to solve this task based on similarities between pairs of vertices. The solution to all these problems are illustrated by means of examples from the real-world, such as the identification of conflicting

factions of tribes in a region of Papua New Guinea, the analysis of the I and II world wars, and the polarization in the voting systems in the European parliament in a given period of time.

2. DEFINITIONS

Throughout this work, we will use the terms graph and network interchangeably. We always consider here that $\#|V| =: n$, and $\#|E| =: m$. We consider only undirected connected signed graphs. Therefore, the adjacency matrix $A(\Sigma) = A$ is a symmetric, square matrix whose entries are $A_{ij} = \pm 1$ if the nodes i and j are connected with an edge of positive or negative sign, respectively, or $A_{ij} = 0$, otherwise.

We will call the spectrum of Σ to the eigenvalues of its adjacency matrix: $Sp(A) = \{\lambda_1, \dots, \lambda_n\}$, where the eigenvalues are in non-increasing order: $\lambda_1 \geq \lambda_2 \geq \dots \geq \lambda_n$. The normalized eigenvector associated with the eigenvalue λ_i is $\psi_i = (\psi_i(1), \dots, \psi_i(n))^T$, and $U = [\psi_1 \ \psi_2 \ \dots \ \psi_n]$ denotes the orthogonal matrix whose columns are the eigenvectors of A . To eliminate ambiguity regarding the direction of each eigenvector, we consistently select ψ_i such that its first component is non-negative, i.e., $\psi_i(1) \geq 0$ for every i . Additionally, throughout all this work, $|A|$ will denote the entrywise absolute of A . Hence, $|A|$ defines an unsigned graph G , called the *underlying graph*, with the same sets of nodes and edges as Σ but where all the edges are positive. A *partition* \mathcal{P} of the node set V is a family of subsets V_1, \dots, V_n that are pairwise disjoint and that cover V . That is, $V_i \cap V_j = \emptyset$ for all i, j , and $\bigcup_j V_j = V$. In the context of this work, we will also use the term *factions* to name the subsets V_1, \dots, V_n . In the case where the set of nodes is partitioned into two factions: $\mathcal{P} = \{V_1, V_2\}$, we will define an indicator function: $I : V \rightarrow \{\pm 1\}$, such that $I(v) = 1$ if $v \in V_1$ and $I(v) = -1$ if $v \in V_2$.

A *walk* is a sequence of (not necessarily different) nodes (v_1, \dots, v_n) such that consecutive nodes are connected by an edge: $(v_i, v_{i+1}) \in E$. If the initial and final nodes coincide in a walk, $v_1 = v_n$, the walk is said to be *closed*. A walk in which every node and edge appear only once is called a *path*. A closed path is known as a *cycle*. The *sign* of the walk/path/cycle is defined as the product of the signs of their edges. Consequently, a *positive* walk/path/cycle contains an even number of negative edges, whereas a *negative* one contains an odd number of negative edges.

A signed graph is said to be *balanced* [30, 40] if every cycle within it is positive or if it does not contain any cycle at all; or equivalently, if every closed walk within it is positive (see figure 2.1(a)). The structural balance theorem proved by Harary [30] connects the concept of balance and that of a partition in a signed graph:

Theorem 1 (Harary). *Let Σ be a signed graph. Then, Σ is balanced if and only if its node set admits a balanced bipartition; i.e., a partition into balanced factions $V = V_1 \cup V_2$ such that every edge connecting nodes of the same faction is positive, while every edge connecting nodes of different factions is negative: $I(v_i) = I(v_j)$ if and only if $A_{ij} > 0$ and $I(v_i) \neq I(v_j)$ if and only if $A_{ij} < 0$.*

This theorem provides a second definition of balance, focusing on partitions instead of cycles. Indeed, in Figure 2.1 we see that a balanced graph admits a balanced partition into two factions (panel (b)), whereas an unbalanced graph does not admit such a partition; i.e., we cannot decide in which faction to place some of the nodes of unbalanced graphs, (panel (e)).

A third way of defining a balanced graph is based on the so-called *switching transformations*. Given a graph Σ with adjacency matrix A , a graph switching is a function $\mathcal{S} : \Sigma \rightarrow \Sigma'$ defined by $\mathcal{S}(A(\Sigma)) = DA(\Sigma)D^{-1}$. The matrix D is a diagonal matrix whose diagonal elements are $+1$ or -1 , and is often called a *switching matrix*. Switching matrices are symmetric and orthogonal; i.e., $D = D^{-1} = D^T$. If two graphs Σ and Σ' can be related by a switching transformation; i.e., $A(\Sigma') = DA(\Sigma)D^{-1}$, we say that these graphs are *switching-equivalent*. Switching-equivalent graphs have the same spectrum, because adjacency matrices related by a switching transformation are similar. The following proposition establishes a connection between structural balance, switching transformations and non-negative matrices:

Proposition 1. [41] *Let Σ be a signed graph with adjacency matrix A . Σ is balanced if and only if there exists a switching matrix D such that $DAD^{-1} = |A|$. Moreover, if such D exists, it has the following form: $D = \text{diag}(I(v_1), \dots, I(v_n))$, where $I(v_j)$ is the indicator function defined in Section 2.*

That is, the switching transformation maps a balanced graph into an unsigned graph, see panel (c) of Figure 2.1. On the other hand, if we apply the switching matrix D to the unbalanced graph of panel (d), a negative edge appears between nodes 1 and 2 (see panel (f) in that Figure). The appearance of this negative edge is a direct consequence of the fact that edge (1,2) is 'frustrated', i.e., we cannot decide a priori in which faction to place its endpoints in the partition given in panel (e).

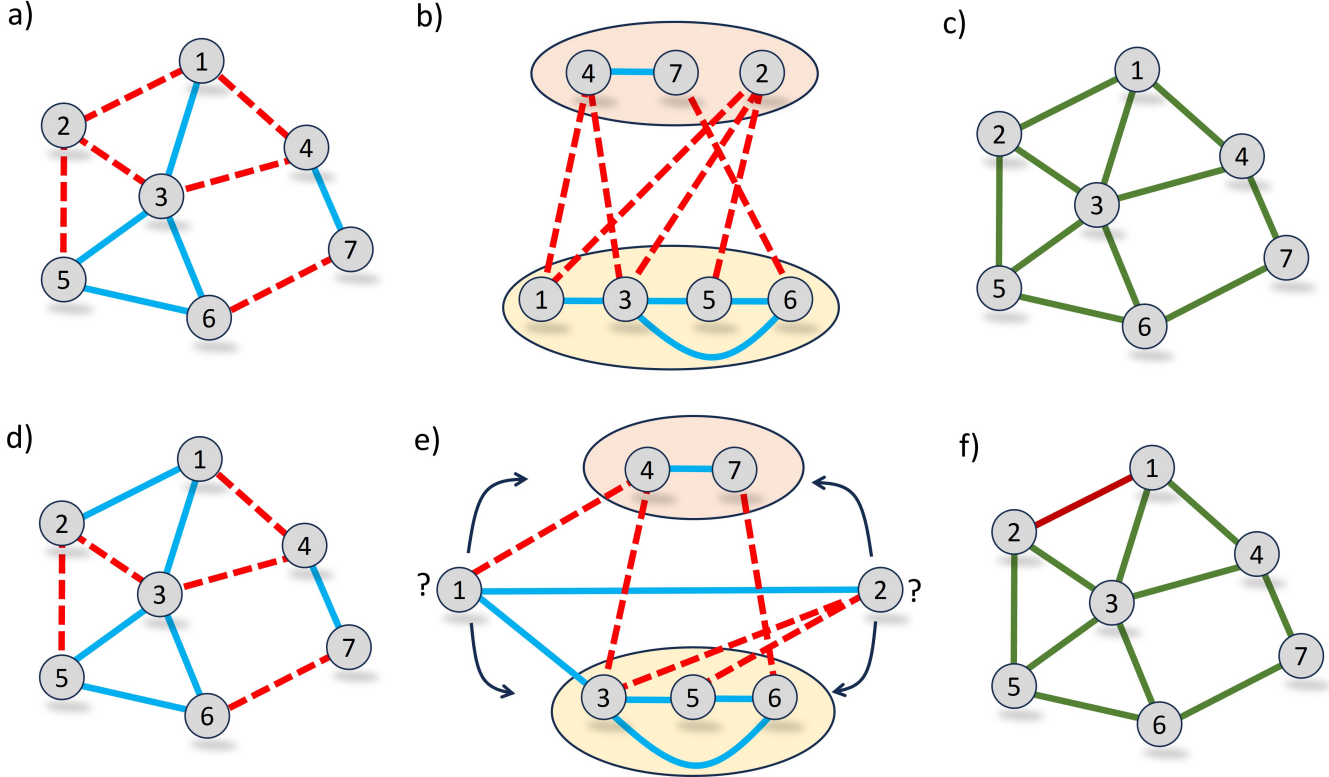


FIG. 2.1: Example of a balanced graph (a), its partition according to Theorem 2.1 (b) and the result of applying the switching transformation described in the text (c). Example of an unbalanced graph (d), an illustration of some problems emerging when trying to apply Theorem 2.1 to this graph (e) as well as the resulting graph of applying the switching transformation mentioned before.

3. RELATED WORKS

Let us start by summarizing the efforts in the literature to consider distances in signed graphs. Spiro [42] defined the length of a path P in Σ as $\sigma(P) = \sum_{e \in E} \sigma(e)$, where $\sigma : E \rightarrow \{1, -1\}$. The shortest path “signed distance” between $u, v \in V$ was defined as $d_{G,\sigma}(u, v) := \min_P |\sigma(P)|$, where the minimum ranges over all uv -paths. Although this “signed distance” may be useful in some graph theoretic problems, it is useless as a pairwise dissimilarity in signed graphs. For instance, if $P = \{(u, v), (v, w)\}$ where $\sigma((u, v)) \neq \sigma((v, w))$, then $d_{G,\sigma}(u, w) = 0$, in spite of the fact that $u \neq w$. Thus, the “signed distance” is not even a distance. More recently, Hameed et al. [43] defined two types of shortest path distances in signed graphs by introducing the following two auxiliary signs: (S1) $\sigma_{max}(u, v) = -1$ if all shortest uv -paths are negative, and +1 otherwise; (S2) $\sigma_{min}(u, v) = +1$ if all shortest uv -paths are positive, and -1 otherwise. The distances are then:

1. $d_{max}(u, v) = \sigma_{max}(u, v)d(u, v) = \max \{\sigma(P(u, v)) : P(u, v) \in \mathbb{P}(u, v)\} d(u, v);$
2. $d_{min}(u, v) = \sigma_{min}(u, v)d(u, v) = \min \{\sigma(P(u, v)) : P(u, v) \in \mathbb{P}(u, v)\} d(u, v),$

where $\mathbb{P}(u, v)$ is the collection of all shortest paths $P(u, v)$ and $d(u, v)$ is the length of the shortest path in the underlying unsigned graph G . To illustrate the drawbacks of this “signed distance” as a similarity measure in signed graphs, let us consider the following two graphs. The first is the signed square $\Sigma_1 = (G_1, \sigma_1)$: $G_1 = (V_1, E_1)$, $V_1 = \{p, q, r, s\}$, $E_1 = \{(p, q), (q, r), (r, s), (s, p)\}$, $\sigma_1 = \{-, +, +, +\}$. The second graph is the signed square $\Sigma_2 = (G_2, \sigma_2)$: $G_2 = (V_2, E_2)$, $V_2 = \{t, u, v, w\}$, $E_2 = \{(t, u), (u, v), (v, w), (w, t)\}$, $\sigma_2 = \{-, +, -, -\}$. The signed distance matrices of these two graphs, which are given in the Appendix, show that their only difference is given by their adjacency relations, which clearly shows their inappropriateness as dissimilarity matrices for signed graphs.

On the other hand, there have also been efforts in the literature to approach the problem of signed graph partition from a computational perspective. The problem is sometimes equated to the “community detection” one, typically applied to unsigned networks, and consisting of the detection of densely connected subsets of vertices in a graph

[44, 45]. The signed version consists of the detection of subsets of nodes connected by positive edges within each subset and negative ones between them. The methods used include the application of objective functions based on the number of negative edges within clusters and of positive ones between clusters and applying clustering methods [46–50], the application of spectral methods based on the adjacency [33, 51, 52] and on the signed Laplacian or its variations [37, 53–57]; and methods based on the modularity measure [58] and its variants [15, 59–61]. Other approaches focus more on the statistical methods for clustering, such as generative graphical models [62], stochastic block-based methods [63, 64], probabilistic mixture-based models [65], and dynamic models [4, 66–68].

The problem of dimensionality reduction in signed graphs has also been treated by using embeddings based either on the signed Laplacian [36, 54, 57], on Hamiltonian functions or similar [69, 70], or on statistics-based embeddings [71]. In the case of the analysis of polarization, although the problem has been extensively studied for unsigned networks [34, 35, 72, 73], it has only been recently reported for signed graphs [10, 69]. Among the methods for predicting missing edges in signed graphs we found approaches based on Laplacian kernels [53], as well as based on balance theory and corresponding indices [28, 74], and other approaches [9, 36, 75].

If we focus on the vertex/graph features used for the analysis of signed graphs more than on the statistical approaches used for signed graph partitioning, we find a series of drawbacks common to several of them. To illustrate some of these problems let us consider the signed pentagon in which only one edge is negative. This example is problematic for the methods based on an objective function, such as the frustration. For instance, in Fig. 3.1 we give five partitions of this graph which minimize the number of frustrated edges. There are no other k -partitions minimizing this objective function. Thus, this problem is undecidable on the basis on frustration-based minimization algorithms. Notice that a frustration index based only of triangles, like it is frequently defined, does not solve this problem as the graph under study has no triangles.

Other approaches use either the leading eigenpair of the signed adjacency matrix or the eigenpair corresponding to the smallest eigenvalue of the signed Laplacian [51, 55]. These methods are inspired on the ones using such eigenvectors in unsigned graphs [76–78]. Although these eigenpairs are unique in unsigned graphs, they are not necessarily so in signed ones. That is, in a signed graph, the multiplicity of the largest eigenvalue of A is not necessarily one, which immediately triggers some problems with these methods. In the example provided in Fig. 3.1

the eigenvalues are: $Sp(A) = \{\varphi, \varphi, 1 - \varphi, 1 - \varphi, -2\}$, where $\varphi = \frac{1 + \sqrt{5}}{2}$ is the golden ratio. Therefore, the largest eigenvalue is degenerated, i.e., it has multiplicity two. The two eigenvectors associated with the eigenvalue λ_1 of multiplicity 2 are: $\psi_1 = [-1, \varphi, \varphi, 1, 0]^T$ and $\psi_2 = [\varphi, -\varphi, -1, 0, 1]^T$, which clearly corresponds to the partitions (b) and (c) in Fig. 2. The vector $\psi_1 + \varphi\psi_2 = [\varphi, -1, 0, 1, \varphi]^T$, which obviously is an eigenvector of A corresponding to λ_1 induces the partition (a) in Fig. 2. Similarly, $-\psi_1 = [1, -\varphi, -\varphi, -1, 0]^T$ and $\varphi\psi_1 + \psi_2 = [0, 1, \varphi, \varphi, 1]^T$ induce the partitions (d) and (e), respectively. Therefore, the use of the eigenvector associated with the largest eigenvalue of the signed adjacency matrix does not allow a good partition in cases where the corresponding eigenvalue has algebraic multiplicity larger than one. Furthermore, for this graph, in which the Laplacian is $L = 2I - A$, where I is the identity matrix, we have a trivial relation of the eigenvalues and eigenvectors of the Laplacian and the adjacency matrices. Thus, the methods based on the least Laplacian eigenpair do not solve either the problems of partitioning this graph.

Methods based on modularity—a measure of the quality of a partition very popular in network analysis—are also known to have several deficiencies for unsigned graphs. There are other measures of the quality of a partition, e.g., Silhouette, Davies-Bouldin, Calinski-Harabasz, etc. [79, 80], and no systematic comparison between them and modularity for (un)signed networks exists. Nonetheless, modularity has been generalized to preserve the probabilistic semantics of the original definition even when the network is weighted, signed, and has self-loops [60]. This generalized modularity is capable to identify the partition (a) in Fig. 3.1 as the one which is “the best”. However, it inherits some of the problems that modularity measure has shown for the case of unsigned graphs, like the resolution limit [81]. For instance, let us build a signed graph formed by k cliques labelled consecutively by $1, 2, \dots, k$, each of size r . Two cliques K_i and K_j are connected by two edges, one positive and the other negative, if and only if $j = i + 1$ or $i = 1$ and $j = k$. The obvious partition is to consider every clique as one cluster. However, for sufficiently big k , modularity identifies the partition which groups pairs of cliques as the best one. This is the signed version of the previously studied resolution problem in unsigned graphs [81].

4. SIGNED WALKS, FACTIONS AND COMMUNICABILITY

In a social system, where the nodes of a network represent social entities and edges represent their social relations, an agreement, i.e., a positive edge, accounts for an affirmation of the state of a node by its positively linked partner. In a similar way, a conflict, i.e., a negative edge, accounts for a negation of the state of a node by its partner. Let a double negation be considered as an affirmation. Then, in a balanced signed graph every walk starting at a node i in the balanced faction V_k and ending at any node j in the same faction represents an affirmation of the states of the

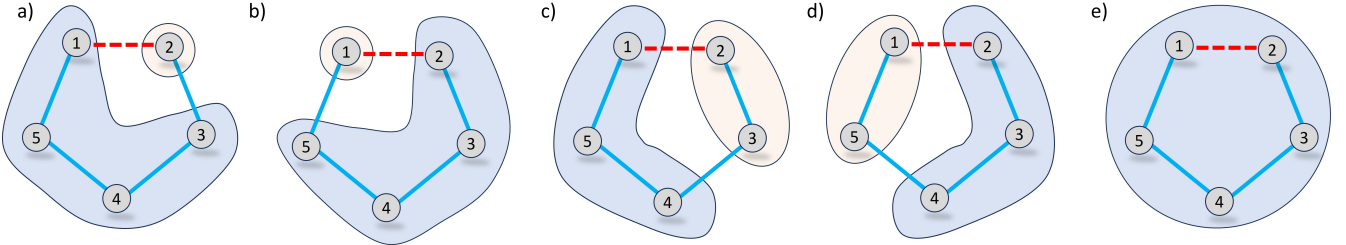


FIG. 3.1: Example of five different signed partitions having the same “frustration” on the pentagon with one negative edge.

two nodes. Let us take for instance the pair of nodes 2 and 4 in the graph (a) of the Figure 2.1. The state of the node 4 is negated by node 1, while the node 2 negates the state of 1, which implies that nodes 2 and 4 affirm their states to each other. On the other hand, the opposite behavior appears when the nodes belong to different (balanced) factions. Let us, for instance, consider the nodes 1 and 7 in the graph (a) of the Figure 2.1. In this case, the path $1 \rightarrow 4 \rightarrow 7$ is a negation of the states of 1 and 7, because 4 negates the state of 1 and 7 affirms the state of 4, ending in negation with 1. It is clear that paths (or walks) ending in negation between the states of their endpoints, are negative, while those mutually affirming the states of the two end points are positive.

In light with the previous discussion, we can say that *two nodes i and j are effective allies if the number of positive walks connecting them exceeds the number of negative walks; otherwise, the nodes are effective enemies*. Moreover, the contribution of a walk should also depend on its length: a short (positive or negative) walk will have significantly more influence than a longer one. Mathematically we can express these ideas as follows. Let $\mu_k^+(i, j)$ be the number of positive walks of length k connecting the nodes i and j and let $\mu_k^-(i, j)$ be number of negative walks of length k connecting the same nodes. Let

$$\Gamma_{ij} = \sum_{k=0}^{\infty} c_k (\mu_k^+(i, j) - \mu_k^-(i, j)), \quad (4.1)$$

where c_k is a penalization factor that decreases as k increases. Then, if $\Gamma_{ij} > 0$ the nodes i and j are effective allies, and if $\Gamma_{ij} < 0$ they are effective enemies and we have the following.

Lemma 1. *Let $i, j \in V$ in a signed graph $\Sigma = (G, \sigma)$ and let $\mu_k^+(i, j)$ and $\mu_k^-(i, j)$ be the number of positive and negative walks of length k between i and j . Then,*

$$\mu_k^+(i, j) - \mu_k^-(i, j) = (A^k)_{ij}. \quad (4.2)$$

We give a complete proof of the previous result in the Appendix accompanying this paper. Let us then consider the following.

Definition 1. *Let Σ be a signed graph with adjacency matrix A . The c -signed communicability $\Gamma_{ij}(A)$ function between nodes i and j is the (i, j) -entry of the matrix function $f(A)$ given by:*

$$\Gamma_{ij}(A) = \sum_{k=0}^{\infty} c_k (A^k)_{ij} = (f(A))_{ij}. \quad (4.3)$$

Here we will consider only the factorial penalization $c_k = (k!)^{-1}$ and simplify the name of Γ_{ij} to signed communicability, although we are talking about the exp-signed communicability. The penalization factor can be adjusted to give more or less weight to longer walks in a signed graph ending up in a plethora of other matrix functions (see [82] for examples).

The term Γ_{ii} accounts for the signed self-communicability of the node i . Notice that in the argot of network theory this term represents a centrality measure of the given node counting its participation in all signed subgraphs of the graph and giving more weight to the smaller than to the longer ones. The following is a difference between the self-communicability and the communicability between two nodes in a signed graph.

Lemma 2. Let $\Sigma = (G, \sigma)$ be a connected signed graph with adjacency matrix A . Let $\Gamma_{ij}(A)$ be the signed self-communicability between the nodes i and j . Then, $\Gamma_{ii}(A) > 0$ for all $i \in V$, while $\Gamma_{ij}(A)$ can take both positive and negative values.

Proof. Let us write $\Gamma_{ij}(A) = \sum_{v=1}^n e^{\lambda_v} \psi_v(i) \psi_v(j)$, which when $i = j$ clearly indicates that $\Gamma_{ii}(A) = \sum_{v=1}^n e^{\lambda_v} \psi_v^2(i) > 0$, while when $i \neq j$ it can also take negative values depending on the sign of $\psi_v(i)$ and $\psi_v(j)$. \square

The matrix exponential was previously mentioned as a potential function for predicting edge signs [36], to define indices that quantify the global [83] and local [13] balance, as well as to quantify polarization in signed graphs [23].

We now arrive at the following result that relates the signed and unsigned communicability (see Appendix for a proof).

Proposition 2. Let Σ be a signed graph with adjacency matrix A . Let $\Gamma_{ij}(A)$ be the communicability between the nodes i and j in the signed graph, and let $\Gamma_{ij}(|A|)$ be the communicability in the unsigned underlying graph of Σ . Then, $|\Gamma_{ij}(A)| \leq \Gamma_{ij}(|A|)$.

A. Communicability of balanced graphs

We start this subsection by proving the following result.

Lemma 3. Let Σ, Σ' be signed graphs with adjacency matrices A, A' respectively. Moreover, assume that Σ and Σ' are switching equivalent; i.e., there is a switching matrix D such that $A' = DAD^{-1}$. Then, the communicability matrices of Σ and Σ' are related by:

$$\Gamma(A') = D\Gamma(A)D^{-1} \quad (4.4)$$

Proof. Let us notice that $(A')^k = DAD^{-1}DAD^{-1} \cdots DAD^{-1} = DA^kD^{-1}$. Proceeding by induction, we find that $(A')^k = DA^kD^{-1}$. Therefore:

$$\Gamma(A') = e^{A'} = \sum_{k=0}^{\infty} \frac{(A')^k}{k!} = \sum_{k=0}^{\infty} \frac{DA^kD^{-1}}{k!} = D \sum_{k=0}^{\infty} \frac{A^k}{k!} D^{-1} = De^A D^{-1} = D\Gamma(A)D^{-1}. \quad (4.5)$$

\square

We are now in conditions of stating the main result of this subsection, whose proof can be found in the Appendix, together with the proofs of its corollaries.

Theorem 2. Let Σ be a signed graph with adjacency matrix A . Then, Σ is balanced if and only if there exists a switching matrix D such that:

$$\Gamma(A) = D\Gamma(|A|)D^{-1}, \quad (4.6)$$

where D is the switching matrix that maps A to $|A|$.

Let us now explore the many consequences of theorem 2. To begin with, let us go back to the inequality of proposition 2: $|\exp(A)| \leq \exp(|A|)$. Theorem 2 allows us to prove that the upper bound of 2 is reached when the network is balanced:

Corollary 1. Let Σ be a signed graph with adjacency matrix A . Σ is balanced if and only if $|\exp(A)| = \exp(|A|)$.

Corollary 2. Let Σ be a signed complete graph. Then, Σ is balanced if and only if for any pair of different vertices i and j , $\Gamma_{ij}(A) = \frac{e^n - 1}{ne}$ or $\Gamma_{ij}(A) = \frac{1 - e^n}{ne}$.

Remark 1. A consequence of the previous Corollary is that all complete graphs which are balanced are isospectral, so that there are $n/2$ (n even) or $(n - 1)/2$ (n odd) isospectral balanced complete graphs. We illustrate in the Figure 4.1 the three existing ones with 6 nodes.

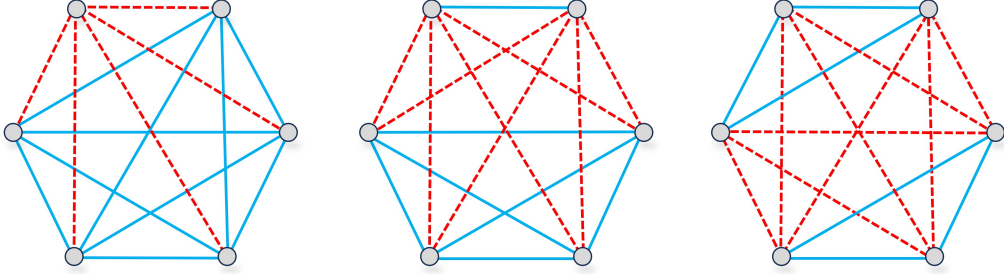


FIG. 4.1: Illustration of the three existing balanced complete graphs with 6 vertices, which are shown here to be isospectral for their adjacency matrices.

5. COMMUNICABILITY GEOMETRY

As we have analyzed in Section 3, the signed versions of the shortest path distance display many problems to use them as similarity measures in data analysis of signed graphs. Thus, it is of great importance to find a distance function that adequately captures the information contained in the negative edges while fulfilling the distance axioms.

Let us start by considering a balanced partition of a balanced signed graph Σ in which $i \in V_1$ and $j \in V_2$. As Σ is balanced, every closed walk starting (and ending) at the node i (respectively at the node j) is always positive. Similarly, every walk starting at node i and ending at node j is negative. Therefore, one will find $\mu_k^-(i, i) = \mu_k^-(j, j) = 0$, as well as $\mu_k^+(i, j) = \mu_k^+(j, i) = 0$. Furthermore, if Σ is unbalanced but “close to balance” (i.e. with a small number of negative cycles), these terms will be nonzero but close to zero for a suitable partition of the node sets into fractions. Therefore, if we add up all those terms accounting for the signs, assuming that $\mu_k^\pm(i, j) = \mu_k^\pm(j, i)$ due to nondirectionality of the graph, the resulting quantity: $(\mu_k^+(i, i) - \mu_k^-(i, i)) + (\mu_k^+(j, j) - \mu_k^-(j, j)) - 2(\mu_k^+(i, j) - \mu_k^-(j, i)) = \Gamma_{ii} + \Gamma_{jj} - 2\Gamma_{ij}$ is expected to be well-defined and positive. Consequently, we introduce the following concept based on the communicability function which, as it has been seen, counts a weighted difference of positive and negative walks in Σ .

Definition 2. Let $\Gamma := \exp(A)$ be the communicability matrix of an undirected signed graph with adjacency matrix A . Then, let us define the term ξ_{ij} between nodes i and j as

$$\xi_{ij} = (\Gamma_{ii} + \Gamma_{jj} - 2\Gamma_{ij})^{1/2}. \quad (5.1)$$

We then have the following:

Theorem 3. ξ_{ij} is a Euclidean distance between the nodes in the signed graph.

The proof of this theorem is included in the Appendix accompanying this work. As usual in the theory of Euclidean distance geometry we define the communicability Euclidean Distance Matrix (EDM) [84, 85] as the matrix whose entries are the squares of the communicability distances:

$$M = s\mathbf{1}^T + \mathbf{1}s^T - 2e^A, \quad (5.2)$$

where $\mathbf{1}$ is an all-ones column vector and $s := \text{diag}(e^A)$. We now state that the communicability EDM is spherical [86] (the formal proof is given in the Appendix). An EDM is called spherical or circum-EDM if the set of points that it represents lie on a hypersphere.

Lemma 4. M is a non-singular spherical EDM.

A potential problem of the (signed) communicability distance is that it is unbounded. Its unboundedness is due to the fact that the terms Γ_{ii} and Γ_{jj} may have an excessive weight in the definition of this distance. Let us provide an example. In the signed graph illustrated in Fig. 5.1 we can see that the balanced partition corresponds to the one which leaves the pendant node in one of the fractions separated from the rest, which form the other fraction (panel (a)). However, the calculation of the signed communicability distance indicates that the pair of nodes forming the negative edge are closer together than the clique to its nearest neighbor. Therefore, any clustering algorithm based on the communicability distance will obtain one cluster formed by the clique and another formed by the two nodes sharing a negative edge (panel (b)), which is not the balanced partition.

In the following we will investigate the terms Γ_{ii} and Γ_{jj} which are the main cause of the bias observed in the (signed) communicability distance. We start by stating the following result which is proved in the Appendix.

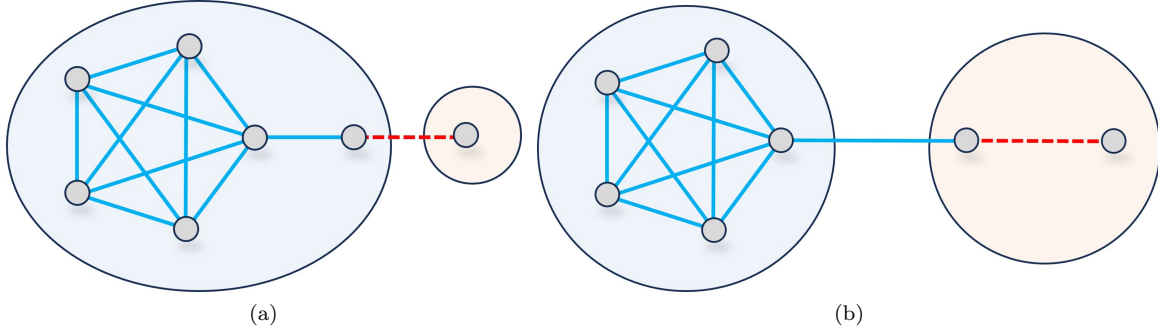


FIG. 5.1: Signed graph used as an example to where the algorithms based on the communicability distance fail to identify the expected balanced partition (a), producing instead the one displayed in panel (b).

Proposition 3. Let $\{x_i\}$ be the generator set formed by the communicability position vectors x_i , where $x_i(k) = \psi_k(i)e^{\lambda_k/2}$, and (λ_k, ψ_k) is the k th eigenpair of the adjacency matrix A of the graph Σ . Moreover, let \hat{x}_i be the communicability position vectors of the underlying unsigned graph and $I(i)$ is the indicator function defined in Section 2. Then, the following assertions hold true:

1. The squared norm of x_i fulfills $\|x_i\|^2 = \Gamma_{ii}$. Moreover, if Σ is balanced, then $\|x_i\| = \|\hat{x}_i\|$.
2. The inner product of x_i and x_j is the signed communicability: $x_i \cdot x_j = \Gamma_{ij}$.
3. $\{x_i\}$ is a basis of an n th dimensional Euclidean space, where n is the number of nodes of the graph.
4. There is only one i for which x_i contains only positive entries.
5. If Σ is balanced, then $x_i = I(i)\hat{x}_i$.
6. If Σ is balanced, then the sign of the first coordinate of every x_i gives the balanced partition of the graph.

One important consequence of Proposition 3 is that the position vectors contain important information to cluster the nodes into factions, even in the unbalanced case. This is exemplified in Figure 5.2, where we plot the four signed triangles in the induced three-dimensional communicability space. The positions of each node correspond to the position vectors x_i . In this example, the sign of the z -component of each x_i informs about the faction to which each node belongs. That is, the $z = 0$ plane separates the nodes into two opposing factions in all cases. In the unsigned graph (top left), all nodes have positive z component, meaning that they all belong to the same faction. Moreover, the value of the z -component could be understood as a measure of the ‘polarization’ of the node, or equivalently, its ‘commitment’ to the faction. In the balanced graph (bottom left), the node with two negative edges has a positive z component, indicating that this node forms a separate faction. Thus, the faction structure determined by the z component coincides exactly with the balanced partition for the balanced graph. This behavior is guaranteed by claim six of Proposition 3 for balanced graphs. Regarding the unbalanced graphs, the z component also returns a sensible partition. In the top right graph, the two nodes connected by a negative edge are assigned to different factions. However, the unbalance in the graph causes the node with negative z -component to have a small magnitude of the z -component; i.e., a small ‘polarization’. Finally, in the bottom right panel, all nodes are equidistant from each other, reflecting the fact that they are automorphically equivalent. The communicability position vectors divide the graph such that one of the nodes has a positive z component, another has a negative one, and finally one has a zero component. Thus, the method successfully detects that the third node cannot belong to either of the two factions.

Because we have previously seen that the magnitude of the communicability position vectors, i.e., the terms Γ_{ii} and Γ_{jj} , introduces a bias in any communicability distance-based partitioning algorithm into factions, we will investigate instead the angle spanned by these vectors.

A. Signed communicability angle

It is straightforward to realize that the angle between the position vectors of two nodes in a signed graph is given by:

$$\cos(\theta_{ij}) = \frac{x_i \cdot x_j}{\|x_i\| \|x_j\|} = \frac{\Gamma_{ij}}{\sqrt{\Gamma_{ii}\Gamma_{jj}}}, \quad (5.3)$$

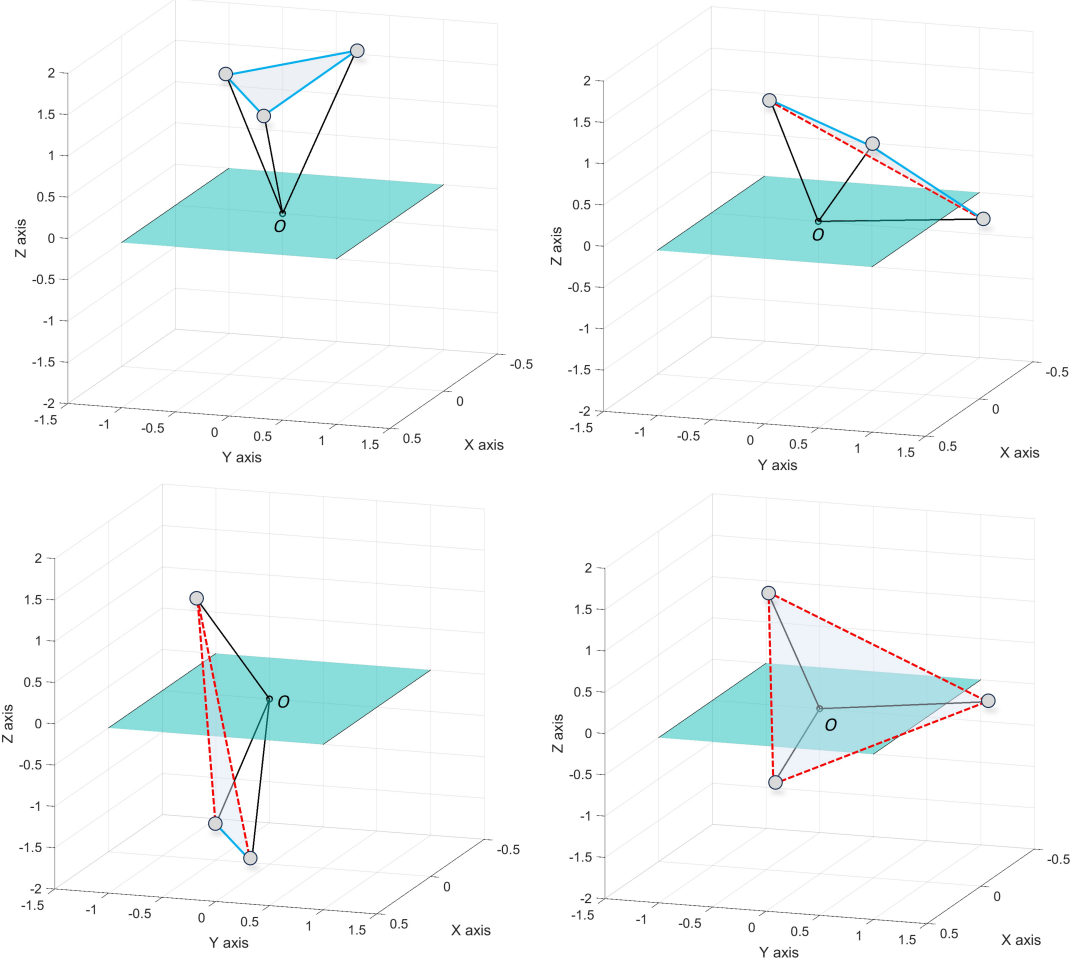


FIG. 5.2: Illustration of the four signed triangles represented in the induced three-dimensional communicability space.

which prompt us to make the following definition.

Definition 3. Let Σ be a signed graph with n nodes and communicability matrix Γ . Let x_i be the position vector defined by $x_i(k) = \psi_k(i)e^{\lambda_k/2}$. Then, the communicability angle θ_{ij} between nodes i and j is defined as the angle between the position vectors x_i and x_j . Mathematically, it is given by the following formula:

$$\theta_{ij} = \cos^{-1} \frac{\Gamma_{ij}}{\sqrt{\Gamma_{ii}\Gamma_{jj}}}. \quad (5.4)$$

We then have the following:

Claim 1. The signed communicability angle is bounded as $0^\circ \leq \theta_{ij} \leq 180^\circ$, where both bounds are attained in balanced complete graphs with sufficiently large number of nodes. The lower bound is attained for pairs of nodes in the same balanced partition and the upper one for pairs of nodes in different balanced partitions.

Remark 2. The previous result, which is proved in the Appendix, illustrates the large separability that the communicability angle achieves between the nodes in a balanced graph, which in the case of complete balanced ones places the nodes in the two antipodes of the hypersphere.

As can be seen in the Fig. C.1 in the Appendix, the signed communicability angle produces a correct partition of the nodes in the graph previously studied in Fig. 5.1. That is, the communicability angle between every pair of vertices in the same partition is positive (see the thick black line in Fig. C.1), and the angle between the vertices at different partitions is negative. Indeed, in the following result we prove that this partition is always possible in signed graphs using the signed communicability angle.

Theorem 4. Let Σ be a balanced graph. Then, the communicability angle between nodes belonging to the same balanced faction is always smaller than the communicability angle between nodes belonging to different balanced factions. Mathematically, if $I(i) = I(j)$ but $I(i) \neq I(k)$, then $\theta_{ij} < \theta_{ik}$, where I is the indicator function defined in Section 2.

Proof. By Theorem 2, we know that, since i and j belong to the same faction, $\Gamma_{ij} > 0$. Given that Γ_{ii}, Γ_{jj} are always positive (Prop. 3.1), it follows that $\cos \theta_{ij} > 0$, so $\theta_{ij} < \pi/2$. On the other hand, since i and k belong to different factions, we have that $\cos(\theta_{ik}) < 0$ and thus $\theta_{ik} > \pi/2$. Combining both inequalities, we find that $\theta_{ij} < \theta_{ik}$. \square

We now proceed to modify the signed communicability distance $\|x_i - x_j\|^2$ to generate a Euclidean distance which is capable of classifying correctly the nodes in a signed graph into its balanced partition. That is, we proceed to normalize the position vectors x_i and x_j to have unit norm in the definition of the signed communicability distance. That is,

$$\left\| \frac{x_i}{\|x_i\|} - \frac{x_j}{\|x_j\|} \right\|^2 = \frac{x_i \cdot x_i}{\|x_i\|^2} + \frac{x_j \cdot x_j}{\|x_j\|^2} - 2 \frac{x_i \cdot x_j}{\|x_i\| \|x_j\|} := d_\theta(i, j). \quad (5.5)$$

In this way we have proved the following.

Proposition 4. The quantity $d_\theta(i, j) = 2 - 2 \cos(\theta_{ij})$ is a squared Euclidean distance between two nodes i and j of Σ .

As we have proved previously that the signed communicability angle solves the problem of classifying the nodes of a graph into its balanced partition, it is obvious that this problem is equally solved by $d_\theta(i, j)$. Therefore, in the following part of this work we proceed to use these metrics to solve some common data science problems, like the partitioning of unbalancing networks into factions.

6. APPLICATIONS

In previous sections, we have seen that the communicability provides several well-defined measures for signed networks: among others, the communicability distance and the communicability angle. These measures can be interpreted as the separation of nodes in an ‘‘alliance space’’. This alliance space tends to group pairs of vertices forming alliances close together, separated from those with whom they maintain antagonistic relations. Moreover, simple transformations, like taking the cosine of the communicability angle, can transform these measures into similarity metrics. In this section, we will explore how these measures can be used in connection with simple statistical and machine-learning techniques to gain novel insights into the structure of empirical signed networks. Specifically, we will focus on applications in (i) network visualization, (ii) detection of factions of allies, (iii) determining a hierarchy of alliances, (iv) dimensionality reduction, and (v) quantification of node polarization. We will exemplify these techniques by using three distinct datasets: firstly, a network of alliances and enmities between tribes in New Guinea (Gahuku-Gama dataset); secondly, a temporal network of international relations throughout the XX century (IR dataset); and finally, a temporal network of voting correlations in the European Parliament (European Parliament dataset).

7. GAHUKU-GAMA TRIBES

To warm up we start by considering the interactions between 15 indigenous tribes located in the Eastern Highlands of the island of Papua New Guinea. The analysis of the ‘‘Gahuku-Gama’’ tribal system has been previously studied by using traditional anthropological techniques [87], and the current analysis exemplifies the use of data analysis based on signed networks in anthropology. One notable aspect of the Gahuku-Gama society is the continuous state of conflict between the different tribes. Violent conflicts erupt every dry season as a consequence of land disputes and accusations of sorcery. Moreover, the tribes often create alliances to gain an advantage against their enemy tribes, forming a complex web of alliances and hostilities. Consequently, the Gahuku-Gama network offers an invaluable testing ground for mathematical theories regarding signed interactions. The geographical distribution of the Gahuku-Gama tribes is shown in Fig. C.2 in the Appendix. Notice that, based only on geographical location, it is difficult to infer which tribes form a cohesive faction.

We begin by showing how the communicability angle matrix can provide a meaningful visualization of the Gahuku-Gama network, and how this can be leveraged to infer antagonistic factions in the network. To do so, we will employ the multidimensional scaling algorithm [88]. This algorithm allows one to embed high-dimensional data into a lower dimensional space, while preserving as faithfully as possible the distances between the data points. In this case, the

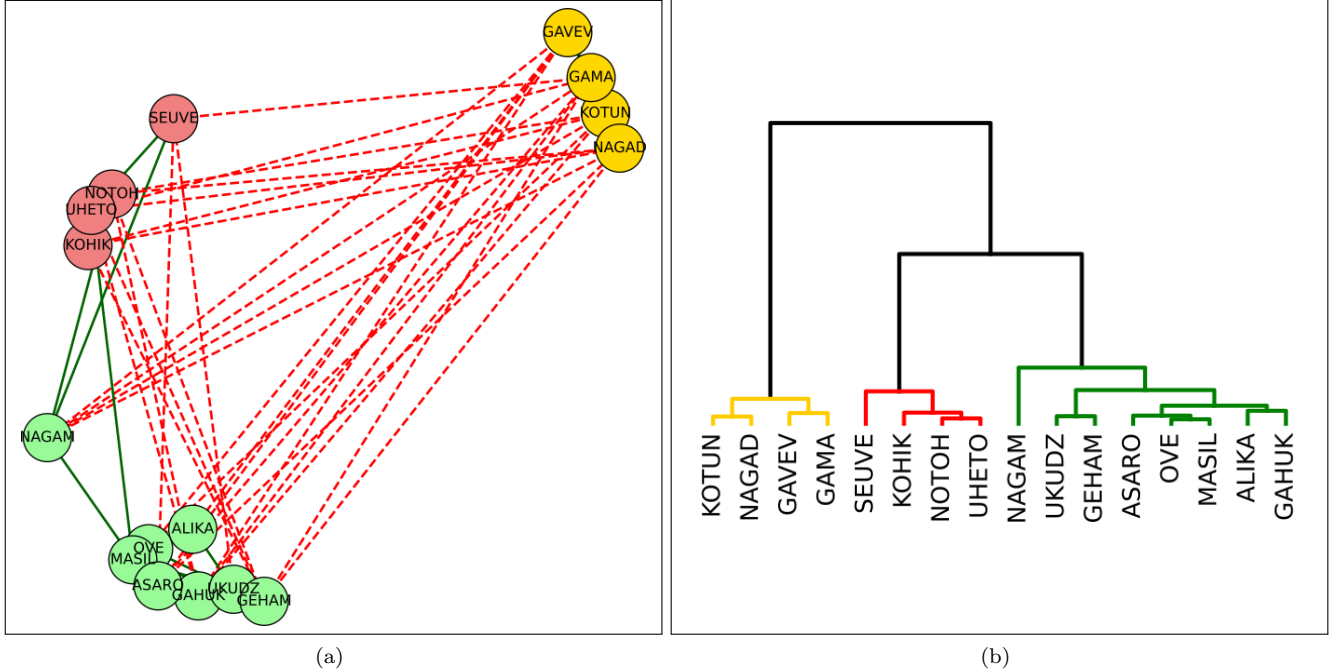


FIG. 7.1: Representation of the partitions of the Gahuku-Gama network, using multidimensional scaling into a two-dimensional space (panel (a)) followed by a K-means clustering algorithm (panel (a)) and hierarchical clustering (panel (b)).

high-dimensional data corresponds to the nodes of the network, while the metric between the nodes is taken to be the communicability angle θ_{ij} . We choose to embed the network into a two-dimensional space so that we can visually inspect its main properties. The resulting embedding is shown in Fig. 7.1. Contrary to the geographical visualization of the network, this communicability-based embedding clearly depicts the factions structure of the network. Firstly, we can see that there is a faction composed by four tribes: GAVEV, GAMA, KOTUN and NAGAD, whose defining characteristic is that they have a common enemy: the NAGAM tribe. The rest of the tribes are split into two additional factions, with the NAGAM tribe acting as a bridge between them. To confirm these qualitative results, we have run a K -means algorithm on the two-dimensional embedding coordinates to detect the cluster structure of the network. The algorithm confirmed that the three-faction structure is indeed the optimal one according to the minimization of the Silhouette index [89]. The clusters returned by the K -means algorithm are indicated through the node colors of Fig. 7.1(a).

Additionally, the communicability angle also provides a simple method for establishing a hierarchy of alliances between the different tribes. By this, we mean a hierarchical structure which provides a ranking of alliances between the pairs of tribes, from the strongest alliance to the weakest one. To achieve this goal, we employ a hierarchical clustering algorithm using the Euclidean distance on the 2D embedding coordinates and Ward linkage [90, 91]. This procedure results in the dendrogram depicted in Fig. 7.1(b), which confirms the three-factions structure that was found both visually and through a clustering algorithm. Moreover, it provides a more nuanced analysis of the emerging alliances between the system of Gahuku-Gama tribes. For example, it ranks the ASARO-OVE-MASIL and NOTOH-UHETO as the two strongest groups of allies. Surprisingly, OVE and ASARO are not connected through an alliance. Therefore, its remarkably strong alliance is an emerging feature that results from their common allies and enemies. This example clearly shows how the effective alliances established through common allies and enmities can have a stronger effect than pairwise alliances. Consequently, local measures such as the classical centrality measures can fail when assessing the hierarchy of alliances, whereas measures which account for the global structure of the signed network, such as the communicability, will provide more accurate results.

8. INTERNATIONAL RELATIONS IN WARTIME

The second analysis focuses on the use of signed networks for data analysis of international relations (IR). We focus here on the first and second World Wars, where the web of IR defines a clear factions structure, which far from being static, was changing over time due to the incorporation of countries to the war effort, cease of hostilities or changing sides. We start by analyzing the international relations during 1914, which corresponds to the beginning of World War I (WWI). The geographical and communicability embeddings of the network are shown in Figs. 8.1(a) and (b). Dark blue and red colors denote the original members of the Entente and Central Powers, respectively. Again, the geographical embedding does not give a clear picture of the faction structure emerging in 1914, whereas the communicability embedding clearly clusters countries according to the faction they joined during WWI. In particular, all the original members of the Entente in 1914 (Serbia, Russia, France, UK, Belgium and Japan) are located in the bottom left corner, while the original members of the Central Powers (Germany, Austria-Hungary and the Ottoman Empire) are located in the upper right corner. More surprisingly, each cluster of the embedded network contains most of the countries that would join the corresponding faction after 1914 (highlighted with light blue and gold colors). In other words, despite the formal neutrality that these countries declared in 1914, the communicability classifies them as aligned with a given faction, which turns out to be the faction they eventually join in future years. The associated hierarchical dendrogram (figure 8.1(c)) confirms these results by grouping most members of the Entente in the left branch and all Central Powers in the right branch.

The two-dimensional embedding discerns a second component present during this period, which is orthogonal to the one formed by the powers at war during WWI. This second axis is composed by Latin American countries, which are well-known to remain neutral during this conflict. Historians have recognized that only about twenty countries remained neutral during WWI and they were mainly Latin American and Northern European ones [92]. It is now clear that the 2D embedding generated with the communicability function of the signed network of IR during this period reveals the existence of two “principal axes” of conflict, in the same way that other statistical techniques, such as the principal component analysis (PCA), discern the principal components of a multivariate dataset.

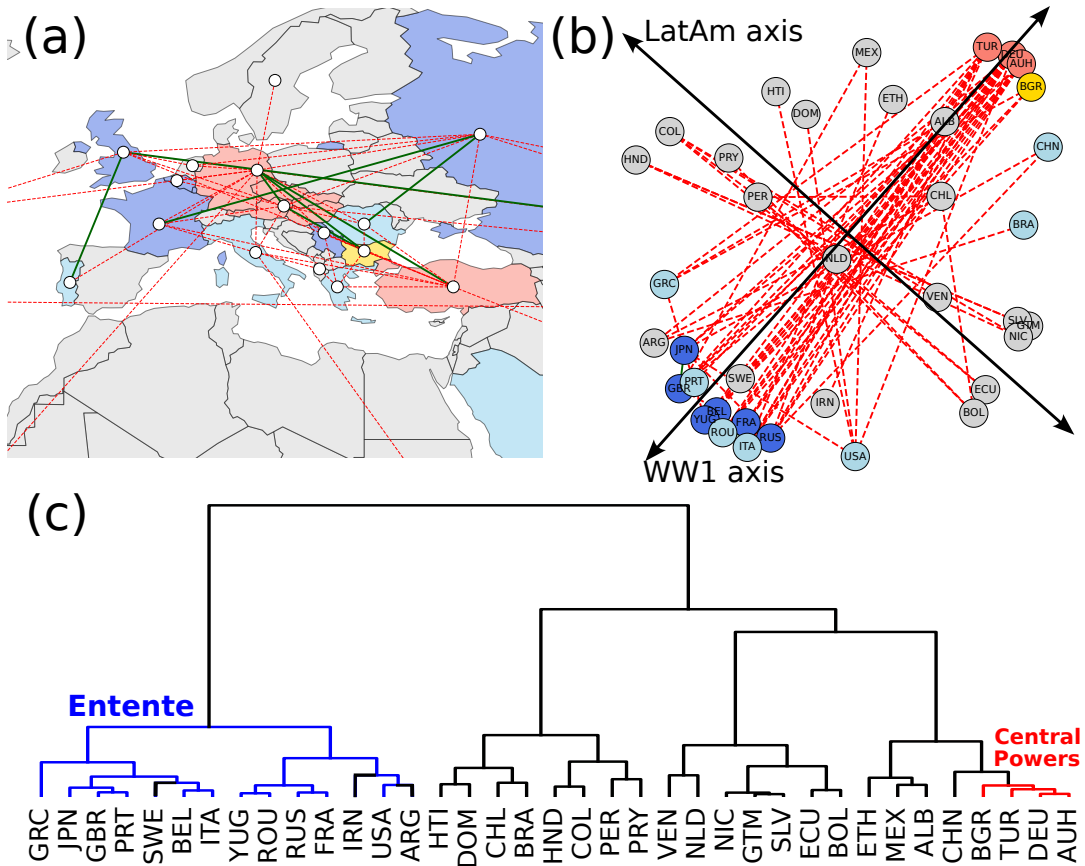


FIG. 8.1: International relations in 1914 represented as a signed graph (a), 2D embedding in the communicability angle space (b), and corresponding dendrogram using ward linkage.

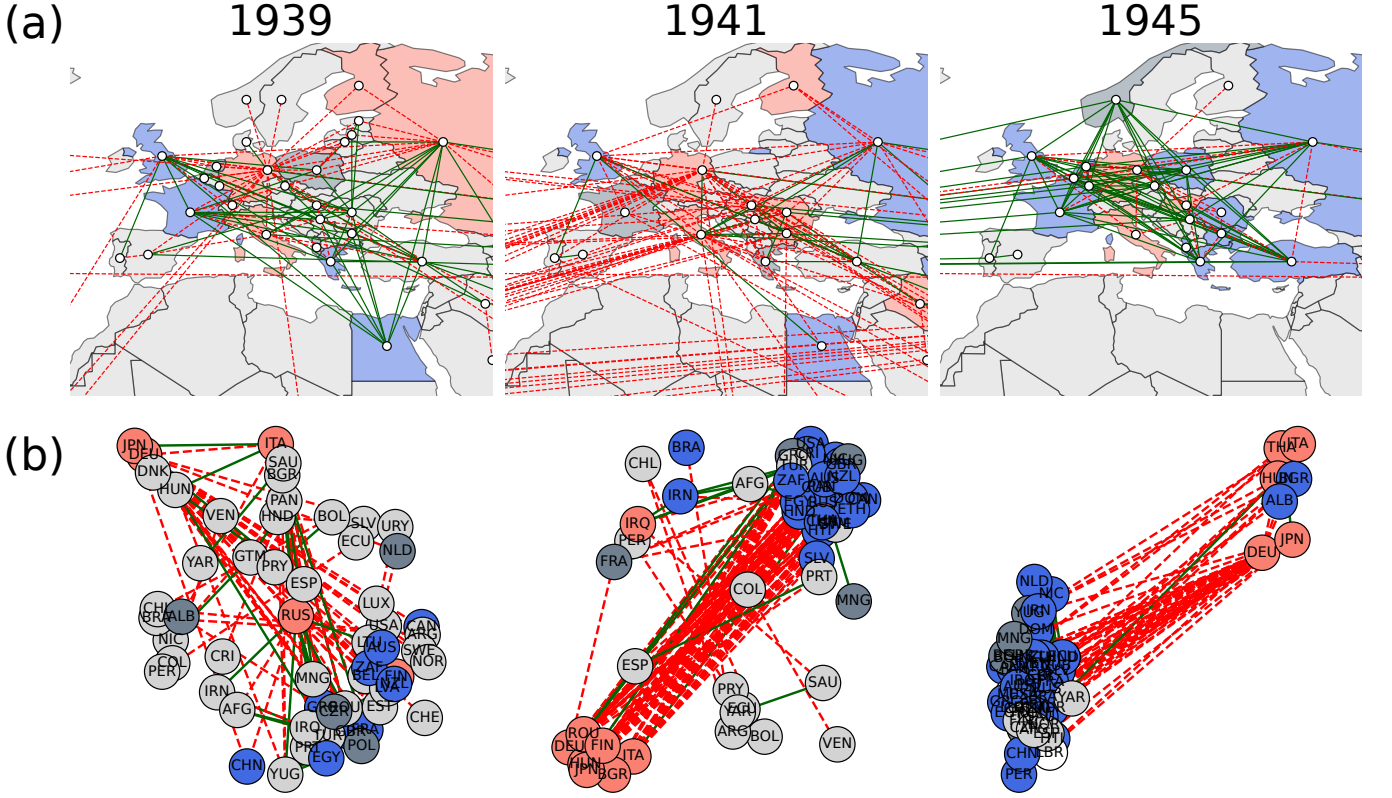


FIG. 8.2: (a) Network of international relations in Europe during World War II, in 1939 (left column), 1941 (middle column) and 1945 (right column). Blue color indicates members of the Allies, red color indicates members of the Axis, and dark grey colors indicate occupied countries. (b) Communicability embedding of corresponding to each of the networks. Same color code as (a).

We now move to the analysis of World war II (WWII), where a more complicated pattern emerges. Instead of a clear division of factions since the beginning of the conflict, one can observe an initially unpolarized network with unclear factions, which becomes more polarized as the war progresses (see Fig. 8.2). One key player in this dynamic is the Union of Soviet Socialist Republics (USSR, iso code RUS). Indeed, in 1939, it occupied the most central position on the embedding. This central position reflects the unorthodox diplomatic choices of the USSR during this year: despite the markedly anti-communist ideology of Nazism, Germany and the USSR signed the Ribbentrop-Molotov non-aggression pact in 1939, which secretly agreed to partition Central and Eastern Europe between them. Thus, the node corresponding to the USSR tends to mark its distance from both the fascist states and Poland's allies, resulting in the observed central position. In 1941, Nazi Germany turned against the USSR and began Operation Barbarossa, resolving the “tension” in the network structure and eventually causing the emergence of a clear faction structure. The factions emerging in 1941 correspond to the Axis Powers and the Allies. Note the unusual positioning of France in the central region, which reflects the Nazi occupation of Northern France and the creation of the collaborationist regime of Vichy France. The faction structure of the network increases further until 1945. In this final year of war, virtually every country had joined one of the two factions, having a clear two-factions structure. The unusual positioning of Albania and Bulgaria reflects that, even though they were nominally Allies in 1945, they had been part of the Axis power until the previous year: Bulgaria was a German ally until a communist coup d'état in 1944 overthrew its Government, while Albania was liberated from German occupation in November 1944. This example illustrates the potentialities of the use of communicability functions of signed networks in the data analysis of historic events, which may be a point in the direction of a more quantitative analysis of history.

9. VOTING SYSTEM AT THE EUROPEAN PARLIAMENT

The third case study on the applications of communicability-based data analysis of signed networks corresponds to its application to political sciences. A way of representing political systems by means of signed networks is by representing by nodes the political actors in a given system and by signed links their affinity or hostility, recorded for

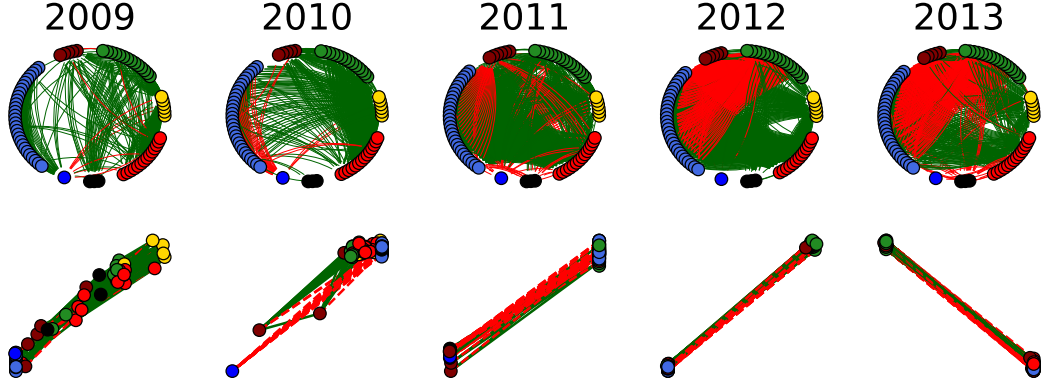


FIG. 9.1: Illustration of the signed networks of the voting system of French members of the European parliament in topics related to agriculture. In the top line we show the networks drawn in a circle and coloring the representative of different groups by different colors. In the bottom line we illustrate the 2-dimensional projection of the same networks based on the communicability geometry, which indicates a clear polarization from 2009 to 2013.

instance by their frequency of common/opposed votes in the system under study. Such “correlation” in their voting pattern can be quantified by means of the Pearson correlation coefficient (other conventions to define the edges can be chosen, see [93]). A frequently appearing feature of these systems is the emergence of *polarization*, where two political factions with completely anticorrelated voting patterns emerge.

Here we study the temporally evolving system obtained from the voting patterns of every pair of representatives in the European Parliament. This dataset comprises the network derived from voting similarities among members of the European Parliament (MEP). We adopt the data analysis protocol outlined in prior works [20, 21]. This protocol entails three steps: (1) Collection of voting records for each MEP across roll-call votes during the 7th term of the European Parliament (2009-2014), sourced from the “It’s Your Parliament (IYP)” website. Our analysis focuses on policy domains pertaining to agriculture, and specifically considers MEPs representing France. This selection is motivated by France’s significant stake in the Common Agricultural Policy (CAP) during this term, given the importance of agriculture to its economy. (2) Calculation of the similarity between all pairs of MEPs within a given political year. This similarity measure is taken to be proportional to the number of times two MEPs voted equally (for example, both voting against a given law) minus the number of times they did not vote equally. To ensure that the similarity lies between -1 and +1, it is divided by the total number of roll-calls of the political year. (3) Application of a thresholding procedure to eliminate weak similarities, thereby converting the dense similarity matrix into a sparse signed network. Further details on this thresholding method can be found in [20]. The nodes of the network belong to one of seven political parties: EPP (center-right, blue color), SD (center-left, red color), ALDE (center, gold color), EFD (right, dark blue color) Greens (environmentalist-left, green color), GUE-NGL (far-left, dark red color), and NI (independent, often far-right, black color). We begin the analysis by embedding the network in a plane, using the embedding technique described in the previous section. In Fig. 9.1, we compare the embedding with a circular layout with the nodes clustered based on their political group. Surprisingly, the political group does not reveal a clear partition of the network, due to the existence of several negative correlations within each Parliamentary group and positive correlations between different ones. In contrast, the communicability embedding unravels several hidden features of this political system. On the other hand, for the communicability embedding, it is remarkable that although the projection of the data is on a two-dimensional space, the vertices tend to align along a straight line, particularly as the time evolves towards 2013. This result contrasts with the latent ideological spaces of other political entities, which seem to have larger dimensions (see e.g. [73]). Furthermore, the distribution of the points along this straight line changes notably from 2009 to 2013. In the first period we find an almost homogeneous distribution of the points along the line, while in 2013 we find that every point is at each of the two extremes. This finding clearly points out toward an increasing tendency in polarization of French representatives in the European parliament.

Therefore, due to the fact that the optimal embedding aligns the nodes along a one-dimensional axis, we can utilize the nodes’ positions on this axis as a measure of its latent polarization. Formally, this corresponds to performing a PCA of the embedding coordinates and taking the first component of every node as its polarization. Moreover, we normalize the components such that they range their values between -1 and +1, so that we can compare node’s polarization for different years. The probability distributions of these latent polarizations, grouped by political affiliation, are illustrated in Fig. C.3. The probability density functions once again show a growing polarization over

time. Interestingly, the representatives of the three largest parties (EPP-SD-ALDE) are mostly grouped within the same factions while the second faction has a volatile composition, with representatives from EFD, the Greens, NI and GUE-NGL coming in and out of it. Let us focus on the Greens, which evolves from a weakly polarized position in 2009 to a large polarization in 2013, where they aligned with EFD, which is traditionally in the opposite faction. In 2013, the European Parliament had to vote for a new Common Agricultural Policy (CAP). This is an extremely important topic in France in which agriculture plays a fundamental role in the economy. In this case, the Greens qualified the new proposal of CAP as unjust from an environmental point of view and voted against it, those aligning with the conservatives of the EFD who were also opposing the law. These results show that the European Parliament dynamics are highly complex and strongly defy the right-left traditional narrative. More importantly, it serves as a clear illustration of the potentialities of the communicability-based analysis of signed networks in political data analysis.

ACKNOWLEDGMENTS

EE thanks Zeev Maoz for sharing data. FDD and EE acknowledge funding from Ministerio de Ciencia e Innovacion, Agencia Estatal de Investigacion Program for Units of Excellences Maria de Maeztu (CEX2021–001164-M/10.13039/501100011033). FDD thanks financial support from MDM–2017–0711 – 20 – 2 funded by MCIN/AEI/10.13039/501100011033 and by FSE invierte en tu futuro, as well as project APASOS (No. PID2021–122256NB–C21). EE also acknowledges funding from project OLGRA (PID2019-107603GB-I00) funded by Spanish Ministry of Science and Innovation.

Appendix A: Mathematical proofs

Lemma 5 (Lemma 4.1). Let $i, j \in V$ in a signed graph $\Sigma = (G, \sigma)$ and let $\mu_k^+(i, j)$ and $\mu_k^-(i, j)$ be the number of positive and negative walks of length k between i and j . Then, $\mu_k^+(i, j) - \mu_k^-(i, j) = (A^k)_{ij}$

Proof of Lemma 4.1. We proceed by induction on k . For $k = 1$, there are only three possibilities: i and j are either connected by a positive edge, by a negative edge, or disconnected. In the first case, $\mu_1^+(i, j) = 1$, $\mu_1^-(i, j) = 0$ and $A_{ij} = 1$. In the second case, $\mu_1^+(i, j) = 0$, $\mu_1^-(i, j) = 1$ and $A_{ij} = -1$. Finally, in the third case $\mu_1^+(i, j) = \mu_1^-(i, j) = 0$ and $A_{ij} = 0$. Thus, in all three cases it is true that $\mu_1^+(i, j) - \mu_1^-(i, j) = A_{ij}$.

Now, let us assume that $\mu_k^+(i, j) - \mu_k^-(i, j) = (A^k)_{ij}$ and prove it for $k + 1$. The induction hypothesis on k implies that the following system holds:

$$\begin{cases} \mu_k^+(i, j) + \mu_k^-(i, j) = (|A|^k)_{ij}; \\ \mu_k^+(i, j) - \mu_k^-(i, j) = (A^k)_{ij}. \end{cases} \quad (\text{A.1})$$

Solving the system, we find that $\mu_k^+(i, j) = \frac{1}{2}[(|A|^k)_{ij} + (A^k)_{ij}]$, $\mu_k^-(i, j) = \frac{1}{2}[(|A|^k)_{ij} - (A^k)_{ij}]$.

We now express the number of positive and negative walks of lengths $k + 1$ in terms of the number of walks of length k . To do so, we observe the following. Given a node l adjacent to j through a positive edge, the number of positive walks of length k from i to l is equal to the number of positive walks of length $k + 1$ from i to j passing through l . On the other hand, if l is connected to j through a negative edge, then the number of negative walks of length k from i to l is equal to the number of negative walks of length $k + 1$ from i to j passing through l . Thus, the total number of positive walks connecting i and j can be found by summing over the neighbors of j , but distinguishing the set of nodes connected to j via positive edges (which we will call $\mathcal{N}^+(j)$) from the set of nodes connected to j via negative edges ($\mathcal{N}^-(j)$):

$$\mu_{k+1}^+(i, j) = \sum_{l \in \mathcal{N}^+(j)} \mu_k^+(i, l) + \sum_{l \in \mathcal{N}^-(j)} \mu_k^-(i, l) \quad (\text{A.2})$$

We can simplify this formula by noticing that the sum over $\mathcal{N}^+(j)$ is equivalent to a sum over all nodes l but multiplying by $\mu_1^+(l, j)$ (after all, the number of positive walks of length one between l and j is one if l and j are connected with a positive edge and zero otherwise). A similar logic can be applied to $\mathcal{N}^-(j)$, obtaining:

$$\mu_{k+1}^+(i, j) = \sum_{l=1}^N \mu_k^+(i, l) \mu_1^+(l, j) + \sum_{l=1}^N \mu_k^-(i, l) \mu_1^-(l, j) \quad (\text{A.3})$$

Now we can apply the expressions for $\mu_k^\pm(i, j)$ to get:

$$\begin{aligned} \mu_{k+1}^+(i, j) &= \sum_l \left(\frac{(|A|^k)_{il} + (A^k)_{il}}{2} \right) \left(\frac{|A|_{lj} + A_{lj}}{2} \right) + \sum_l \left(\frac{(|A|^k)_{il} - ((A^k)_{il})}{2} \right) \left(\frac{|A|_{lj} - A_{lj}}{2} \right) = \\ &= \frac{1}{2} \sum_l [(|A|^k)_{il} |A|_{lj} + (A^k)_{il} A_{lj}] = \\ &= \frac{1}{2} [(|A|^{k+1})_{ij} + (A^{k+1})_{ij}] \end{aligned}$$

In the same manner, $\mu_{k+1}^-(i, j)$ can be written as:

$$\begin{aligned} \mu_{k+1}^-(i, j) &= \sum_{l=1}^N \mu_k^+(i, l) \mu_1^-(l, j) + \sum_{l=1}^N \mu_k^-(i, l) \mu_1^+(l, j) \\ &= \frac{1}{4} \sum_l \left(\frac{(|A|^k)_{il} + (A^k)_{il}}{2} \right) \left(\frac{|A|_{lj} - A_{lj}}{2} \right) + \sum_l \left(\frac{(|A|^k)_{il} - (A^k)_{il}}{2} \right) \left(\frac{|A|_{lj} + A_{lj}}{2} \right) = \\ &= \frac{1}{2} \sum_l [(|A|^k)_{il} |A|_{lj} - (A^k)_{il} A_{lj}] = \frac{1}{2} [(|A|^{k+1})_{ij} - (A^{k+1})_{ij}] \end{aligned}$$

Finally, subtracting:

$$\mu_{k+1}^+(i, j) - \mu_{k+1}^-(i, j) = \frac{1}{2} [(|A|^{k+1})_{ij} + (A^{k+1})_{ij} - (|A|^{k+1})_{ij} + (A^{k+1})_{ij}] = (A^{k+1})_{ij},$$

which is the induction hypothesis for $k + 1$. Thus, by the induction principle, our claim is true for all k . \square

Proposition 5 (Proposition 4.4). *Let Σ be a signed graph with adjacency matrix A . Let $\Gamma_{ij}(A)$ be the communicability between the nodes i and j in the signed graph, and let $\Gamma_{ij}(|A|)$ be the communicability in the unsigned underlying graph of Σ . Then, $|\Gamma_{ij}(A)| \leq \Gamma_{ij}(|A|)$.*

Proof of Proposition 4.4. Let us write

$$|\Gamma_{ij}(A)| = |(e^A)_{ij}| = \left| \sum_{k=0}^{\infty} \frac{1}{k!} (A^k)_{ij} \right| \leq \sum_{k=0}^{\infty} \frac{1}{k!} |A^k|_{ij}. \quad (\text{A.4})$$

On the other hand:

$$|A^k|_{ij} = \left| \sum_{l_1, \dots, l_{k-1}} A_{il_1} A_{l_1 l_2} \dots A_{l_{k-1} j} \right| \leq \sum_{l_1, \dots, l_{k-1}} |A|_{pl_1} |A|_{l_1 l_2} \dots |A|_{l_{k-1} j} = |A|_{ij}^k. \quad (\text{A.5})$$

Combining the last two inequalities, we obtain $|\Gamma_{ij}(A)| \leq \sum_k \frac{1}{k!} |A|_{ij}^k = \Gamma_{ij}(|A|)$. \square

Theorem 5 (Theorem 4.6). *Let Σ be a signed graph with adjacency matrix A . Then, Σ is balanced if and only if there exists a switching matrix D such that:*

$$\exp(A) = D \exp(|A|) D^{-1}, \quad (\text{A.6})$$

where D is the switching matrix that maps A to $|A|$.

Proof of Theorem 4.6. We begin by proving the necessary condition. Assume that Σ is balanced. Then, by Prop. 2.2, there is some matrix D such that $A = D|A|D^{-1}$. Consequently, according to Lemma 4.5 we have that $\exp(A) = D \exp(|A|) D^{-1}$.

For the sufficient condition, we assume that $\exp(|A|) = D^{-1} \exp(A) D$. We then proceed to prove that Σ is balanced. Let us use the Taylor series expansion of the communicability, to get:

$$\sum_{k=0}^{\infty} \frac{|A|^k}{k!} = \sum_{k=0}^{\infty} \frac{D^{-1} A^k D}{k!} \Rightarrow \sum_{k=0}^{\infty} \frac{1}{k!} (|A|^k - D^{-1} A^k D) = 0. \quad (\text{A.7})$$

We will now prove that every term inside the parenthesis has the same sign, so that the sum is zero if and only if every term within it is exactly zero. Using the fact that D is diagonal and $D = D^{-1}$, we can write each term within the parenthesis as $|A|_{ij}^k - D_{ii} D_{jj} (A^k)_{ij}$. Now, we distinguish two cases. On the one hand, if $D_{ii} D_{jj} = +1$, then the expression reduces to $|A|_{ij}^k - (A^k)_{ij}$, and since $|A|^k \geq A^k$ for any k , the term is non-negative for every k . On the other hand, if $D_{ii} D_{jj} = -1$, the term becomes $|A|_{ij}^k + (A^k)_{ij}$, where A^k could contain negative entries. However, in the proof of Proposition 4.4, we showed that $|A|_{ij}^k \geq |A^k|_{ij}$, which implies that the sum is non-negative for every k even if A^k contains negative entries. Therefore, we have shown that each term in the sum is greater or equal to zero, and as a consequence the sum is zero if and only if

$$|A|^k = D^{-1} A^k D, \quad (\text{A.8})$$

for every k . In particular, taking $k = 1$ and using $D = D^{-1}$, we get

$$|A| = DAD^{-1}, \quad (\text{A.9})$$

which according to Prop. 2.2 is a sufficient condition for Σ to be a balanced graph. Moreover, this also proves that D is indeed the balanced switching matrix that maps A to $|A|$, completing the proof. \square

Corollary 3 (Corollary 4.7). *Let Σ be a signed graph with adjacency matrix A . Σ is balanced if and only if $|e^A| = e^{|A|}$.*

Proof of Corollary 4.7. If Σ is balanced, then $(e^A)_{ij} = D_{ii} (e^{|A|})_{ij} D_{jj}$ by Theorem 4.6. Taking absolute values in both sides and using that $|D_{ii}| = 1$ for all i , we get $|(e^A)_{ij}| = (e^{|A|})_{ij}$, which is the same as $|\exp(A)| = \exp(|A|)$.

On the other hand, if Σ is unbalanced, then there are two nodes i and j connected through both a positive and a negative path [30, 39]. Let us denote the lengths of the positive and negative paths by l_+ and l_- , respectively. Recall that A^k counts the difference between positive and negative walks of length k , while $|A|^k$ counts the number of walks, regardless of sign. Moreover, eq. (A.5) implies that $-|A|_{ij}^k \leq A_{ij}^k \leq |A|_{ij}^k$. The first inequality is reached if and only

if all walks between i and j are negative, whereas the second one is reached if and only if all such walks are positive. Therefore, the existence of a negative path of length l_- between nodes i and j implies that $A_{ij}^{l_-} < |A|_{ij}^{l_-}$; and the existence of the positive path of length l_+ implies $A_{ij}^{l_+} > -|A|_{ij}^{l_+}$. This means that:

$$-\sum_{k=0}^{\infty} \frac{|A|_{ij}^k}{k!} < \sum_{k=0}^{\infty} \frac{A_{ij}^k}{k!} < \sum_{k=0}^{\infty} \frac{|A|_{ij}^k}{k!}, \quad (\text{A.10})$$

which implies that $-(e^{|A|})_{ij} < (e^A)_{ij} < (e^{|A|})_{ij}$. This means that $|e^A| \neq e^{|A|}$, thus completing the proof. \square

Corollary 4 (Corollary 4.8). *Let Σ be a signed complete graph. Then, Σ is balanced if and only if for any pair of different vertices i and j , $\Gamma_{ij}(A) = \frac{e^n - 1}{ne}$ or $\Gamma_{ij}(A) = \frac{1 - e^n}{ne}$.*

Proof of Corollary 4.8. We begin by noting that, for an unsigned complete graph, the communicability between any pair of distinct nodes is $\Gamma_{ij}(|A|) = \frac{e^n - 1}{ne}$. If Σ is balanced, it admits a balanced switching matrix D and we can apply Theorem 4.6. Moreover, if i and j belong to different factions, the elements D_{ii} and D_{jj} have opposite sign, and thus $\Gamma_{ij}(A) = -\Gamma_{ij}(|A|) = -\frac{e^n - 1}{ne}$.

We now prove the sufficient condition, which is equivalent to proving that if Σ is unbalanced, then $|\Gamma_{ij}(A)| \neq \frac{e^n - 1}{ne}$. If Σ is unbalanced, then according to Corollary 4.7, there is a pair (i, j) such that $|\Gamma_{ij}(A)| < \Gamma_{ij}(|A|)$. Thus, $|\Gamma_{ij}(A)| \neq \frac{e^n - 1}{ne}$. \square

Theorem 6 (Theorem 5.2). *ξ_{ij} is a Euclidean distance between the corresponding nodes in the signed graph.*

Proof of Theorem 5.2. We begin the proof by considering the spectral decomposition of Γ_{ij} :

$$\Gamma_{ij} = \sum_k \psi_k(i)\psi_k(j)e^{\lambda_k}. \quad (\text{A.11})$$

Substituting this expression in the definition of ξ_{ij} and squaring both sides, we get:

$$\xi_{ij}^2 = \sum_k e^{\lambda_k} (\psi_k(i) - \psi_k(j))^2. \quad (\text{A.12})$$

Let $\varphi_i = [\psi_1(i) \cdots \psi_n(i)]^T$, then we can write

$$\xi_{ij}^2 = (\varphi_i - \varphi_j)^T e^A (\varphi_i - \varphi_j), \quad (\text{A.13})$$

where Λ is the diagonal matrix of eigenvalues of A . Then, we can write

$$\xi_{ij}^2 = \left(e^{\Lambda/2} \varphi_i - e^{\Lambda/2} \varphi_j \right)^T \left(e^{\Lambda/2} \varphi_i - e^{\Lambda/2} \varphi_j \right), \quad (\text{A.14})$$

which, by defining $x_i := e^{\Lambda/2} \varphi_i$, is expressed as

$$\begin{aligned} \xi_{ij}^2 &= (x_i - x_j)^T (x_i - x_j) \\ &= \|x_i - x_j\|^2. \end{aligned} \quad (\text{A.15})$$

\square

Lemma 6 (Lemma 5.3). *The matrix $M = s\mathbf{1}^T + \mathbf{1}s^T - 2e^A$, with $s = \text{diag}(e^A)$ and $\mathbf{1}$ a vector of ones, is a non-singular spherical EDM.*

Proof of Lemma 5.3. Here we follow Gower [84] who proved that the points that generate the matrix M lie on the surface of a hypersphere if and only if $\mathbf{1}^T M^{-1} \mathbf{1} \neq 0$. Thus, we have to prove that M^{-1} exists. We first use the Sherman-Morrison-Woodbury [94] formula to have

$$\begin{aligned}
M^{-1} &= ((-2e^A + \mathbf{1}s^T) + s\mathbf{1}^T)^{-1} \\
&= -\frac{1}{2}e^{-A} - \frac{(e^{-A}\mathbf{1}s^Te^{-A})}{4 - 2s^Te^{-A}\mathbf{1}} - \frac{\left(-\frac{1}{2}e^{-A} - \frac{(e^{-A}\mathbf{1}s^Te^{-A})}{4 - 2s^Te^{-A}\mathbf{1}}\right)s\mathbf{1}^T\left(-\frac{1}{2}e^{-A} - \frac{(e^{-A}\mathbf{1}s^Te^{-A})}{4 - 2s^Te^{-A}\mathbf{1}}\right)}{1 + \mathbf{1}^T\left(-\frac{1}{2}e^{-A} - \frac{(e^{-A}\mathbf{1}s^Te^{-A})}{4 - 2s^Te^{-A}\mathbf{1}}\right)s} \\
&= -\frac{1}{2}e^{-A} - \frac{ab}{4 - 2\varepsilon} - \frac{\left(-\frac{1}{2}b^T - \frac{ac}{4 - 2\varepsilon}\right)\left(-\frac{1}{2}a^T - \frac{db}{4 - 2\varepsilon}\right)}{1 + \left(-\frac{1}{2}\varepsilon - \frac{dc}{4 - 2\varepsilon}\right)},
\end{aligned} \tag{A.16}$$

where $a = e^{-A}\mathbf{1}$, $b = s^Te^{-A}$, $c = s^Te^{-A}s$, $d = \mathbf{1}^Te^{-A}\mathbf{1}$, and $\varepsilon = s^Te^{-A}\mathbf{1}$. We then have

$$M^{-1} = -\frac{1}{2}e^{-A} + \frac{caa^T - (\varepsilon - 2)b^Ta^T - (\varepsilon - 2)ab + db^Tb}{2(cd - (\varepsilon - 2)^2)}. \tag{A.17}$$

We now prove that $cd - (\varepsilon - 2)^2 \neq 0$ for which we start by noticing that $c \geq \varepsilon$, with equality if and only if $s = \mathbf{1}$. This equality holds only if the graph is trivial, which is excluded here as the graphs are connected. Therefore,

$$-\varepsilon^2 + cd + 4\varepsilon - 4 > -\varepsilon^2 + (d + 4)\varepsilon - 4 > 0, \tag{A.18}$$

where the last inequality is obvious from the roots of the quadratic equation.

We now obtain $\mathbf{1}^T M^{-1} \mathbf{1}$, as

$$\mathbf{1}^T M^{-1} \mathbf{1} = -\frac{1}{2}d - \frac{d\varepsilon}{4 - 2\varepsilon} - \frac{\left(-\frac{1}{2}\varepsilon - \frac{dc}{4 - 2\varepsilon}\right)\left(-\frac{1}{2}d - \frac{d\varepsilon}{4 - 2\varepsilon}\right)}{1 + \left(-\frac{1}{2}\varepsilon - \frac{dc}{4 - 2\varepsilon}\right)} \tag{A.19}$$

$$= \frac{2d}{cd - (\varepsilon - 2)^2}. \tag{A.20}$$

Because $d = \mathbf{1}^Te^{-A}\mathbf{1}$ is the sum of all the entries of e^{-A} and $A \neq 0$ (because the graph is not trivial), we have that $d > 0$. Then, because we have proved before that $cd - (\varepsilon - 2)^2 > 0$, we have proved that M is a nonsingular spherical EDM. \square

Proposition 6 (Proposition 5.4). *Let $\{x_i\}$ be the generator set formed by the communicability position vectors x_i , where $x_i(k) = \psi_k(i)e^{\lambda_k/2}$, and (λ_k, ψ_k) is the k th eigenpair of the adjacency matrix A of the graph Σ . Moreover, let \hat{x}_i be the communicability position vectors of the underlying unsigned graph and $I(i)$ is the indicator function defined in Section 2. Then, the following assertions hold true:*

1. *The squared norm of x_i fulfills $\|x_i\|^2 = \Gamma_{ii}(A)$. Moreover, if Σ is balanced, then $\|x_i\| = \|\hat{x}_i\|$.*
2. *The inner product of x_i and x_j is the signed communicability: $x_i \cdot x_j = \Gamma_{ij}(A)$.*
3. *$\{x_i\}$ is a basis of an n th dimensional Euclidean space, where n is the number of nodes of the graph.*
4. *There is only one i for which x_i contains only positive entries.*
5. *If Σ is balanced, then $x_i = I(i)\hat{x}_i$.*
6. *If Σ is balanced, then the sign of the first coordinate of every x_i gives the balanced partition of the graph.*

Proof of Proposition 5.4. The first two assertions come from the fact that

$$x_i \cdot x_j = \sum_k \psi_k(i) e^{\lambda_k/2} \psi_k(j) e^{\lambda_k/2} = \Gamma_{ij}(A). \quad (\text{A.21})$$

An equivalent argument leads to the following relation for the underlying unsigned graph: $\hat{x}_i \cdot \hat{x}_j = \Gamma_{ij}(|A|)$. Finally, since Σ is balanced, we apply Theorem 4.6 to the diagonal entries of $\Gamma(A)$, obtaining $\Gamma_{ii}(A) = \Gamma_{ii}(|A|)$; i.e., $\|x_i\| = \|\hat{x}_i\|$.

To prove the statement 3 let us define X to be the matrix whose columns are the vectors x_j . It is easy to see that $X = e^{\Lambda/2} U^T$, whose entries are:

$$X_{ij} = x_j(i) = \psi_i(j) e^{\lambda_i/2} = \sum_k \delta_{ik} e^{\lambda_k/2} \psi_k(j) = \sum_k (e^{\Lambda/2})_{ik} U_{jk} = (e^{\Lambda/2} U^T)_{ij} \quad (\text{A.22})$$

Now, we apply the properties of determinants to find that $\det(X) = \det(e^{\Lambda/2}) \det(U^T)$. On the one hand, U is not singular because the eigenvectors of symmetric matrices form a basis and change-of-basis matrices are never singular. Because $e^{\Lambda/2}$ is not singular it follows that $\det(X) \neq 0$, so X is not singular and the columns form a set of linear independent vectors. Since $\dim(X) = n$, this set of linearly independent vectors is maximal in \mathbb{R}^n ; i.e., a basis.

Let us now prove the fourth statement. We begin by proving that at least one x_i contains only positive components. Since the eigenvectors ψ_j of A are defined up to sign, one can choose the sign of each eigenvector so that the i th component of every eigenvector is positive. Therefore, $x_i = (\psi_1(i)e^{\lambda_1/2}, \psi_2(i)e^{\lambda_2/2}, \dots)^T$ only contains positive entries. To prove that there cannot be two vectors x_i, x_j with only positive components, first observe that set of vectors of the form $(\psi_1(i), \psi_2(i), \dots)^T$ forms an orthonormal basis. Suppose x_i contains only positive entries. Then, $(\psi_1(i), \psi_2(i), \dots)^T$ also contains only positive entries. Hence, to ensure orthogonality, every vector of the form $(\psi_1(j), \psi_2(j), \dots)^T$ with $j \neq i$ must contain at least one negative entry. The same entry will also be negative in the vector $(\psi_1(i)e^{\lambda_1/2}, \psi_2(i)e^{\lambda_2/2}, \dots)^T$. But this vector is x_j , so every x_j with $j \neq i$ contains a negative entry.

To prove the fifth statement let us begin by relating the eigenvectors of A and $|A|$ when Σ is balanced. Since Σ is balanced, proposition 2.1 relates A and $|A|$ through $|A| = DAD$. Let $\hat{\psi}_j$ be an eigenvector of $|A|$. Then, $\lambda_j \hat{\psi}_j = |A| \hat{\psi}_j = DAD\hat{\psi}_j \Rightarrow A(D\hat{\psi}_j) = \lambda_j(D\hat{\psi}_j)$; i.e., $D\hat{\psi}_j$ is an eigenvector of A with the same eigenvalue as $|A|$. In other words, the eigenvectors ψ_j and $\hat{\psi}_j$ are related by $\psi_j = D\hat{\psi}_j$, and their components fulfill $\psi_j(i) = D_{ii}\hat{\psi}_j(i)$. Now, we substitute this last expression into the definition of x_i :

$$x_i(j) = \psi_j(i) e^{\lambda_j/2} = D_{ii}\hat{\psi}_j(i) e^{\lambda_j/2} = D_{ii}\hat{x}_i(j), \quad (\text{A.23})$$

where \hat{x}_i is the communicability position vector of $|A|$. Since this last equation is valid for all j and $D_{ii} = I(i)$, we conclude that $x_i = I(i)\hat{x}_i$.

Finally, the sixth statement is a consequence of the fact that since $|A|$ is non-negative, the Perron-Frobenius theorem asserts that the principal eigenvector of $\hat{\psi}_1$ only contain positive entries. Consequently, $\hat{x}_i(1) = \hat{\psi}_1(i)e^{\lambda_1/2}$ is positive. Now, because Σ is balanced, we can use statement 5 to relate $x_i(1)$ and $\hat{x}_i(1)$ through $x_i(1) = I(i)\hat{x}_i(1)$, and therefore $\text{sgn}(x_i(1)) = I(i)$. In other words, the sign of $x_i(1)$ tells us the faction to which node 1 belongs. \square

Claim 2 (Claim 5.6). *The signed communicability angle is bounded as $0^\circ \leq \theta_{ij} \leq 180^\circ$, where both bounds are attained in balanced complete graphs with sufficiently large number of nodes. The lower bound is attained for pairs of nodes in the same balanced partition and the upper one for pairs of nodes in different balanced partitions.*

Proof of Claim 5.6. Let Σ be a signed complete graph with balanced partition given by the sets V_1 and V_2 . Then, it was previously proved (Corollary 4.8) that for $i \neq j$

$$\Gamma_{ij} = \begin{cases} \frac{e^n - 1}{ne} & I(i) \neq I(j) \\ \frac{1 - e^n}{ne} & I(i) = I(j) \end{cases} \quad (\text{A.24})$$

It can be seen that $\Gamma_{ii} = \frac{e^{n-1} + (n-1)e^{-1}}{n}$ for any $i \in V$. Therefore,

$$\theta_{ij} = \cos^{-1} \frac{\Gamma_{ij}}{\sqrt{\Gamma_{ii}\Gamma_{jj}}} = \begin{cases} \cos^{-1} \left(\frac{e^n - 1}{e^n + n - 1} \right) & I(i) = I(j) \\ \cos^{-1} \left(-\frac{e^n + 1}{e^n + n - 1} \right) & I(i) \neq I(j) \end{cases} \quad (\text{A.25})$$

which for n sufficiently large is

$$\lim_{n \rightarrow \infty} \theta_{ij} = \cos^{-1} \frac{\Gamma_{ij}}{\sqrt{\Gamma_{ii}\Gamma_{jj}}} = \begin{cases} \cos^{-1}(1) & I(i) = I(j) \\ \cos^{-1}(-1) & I(i) \neq I(j) \end{cases} \quad (\text{A.26})$$

□

Appendix B: Signed distance matrices

The signed distance matrices based on Hammed et al. definition [43] for the two graphs discussed in Section 3 are:

$$D^{max}(\Sigma_1) = \begin{bmatrix} 0 & -1 & 2 & 1 \\ -1 & 0 & 1 & 2 \\ 2 & 1 & 0 & 1 \\ 1 & 2 & 1 & 0 \end{bmatrix}, D^{max}(\Sigma_2) = \begin{bmatrix} 0 & -1 & 2 & 1 \\ -1 & 0 & 1 & 2 \\ 2 & 1 & 0 & -1 \\ -1 & 2 & -1 & 0 \end{bmatrix}, \quad (\text{B.1})$$

$$D^{min}(\Sigma_1) = \begin{bmatrix} 0 & -1 & -2 & 1 \\ -1 & 0 & 1 & -2 \\ -2 & 1 & 0 & 1 \\ 1 & 2 & 1 & 0 \end{bmatrix}, D^{min}(\Sigma_2) = \begin{bmatrix} 0 & -1 & -2 & 1 \\ -1 & 0 & 1 & -2 \\ -2 & 1 & 0 & -1 \\ -1 & -2 & -1 & 0 \end{bmatrix}. \quad (\text{B.2})$$

Appendix C: Supplementary figures

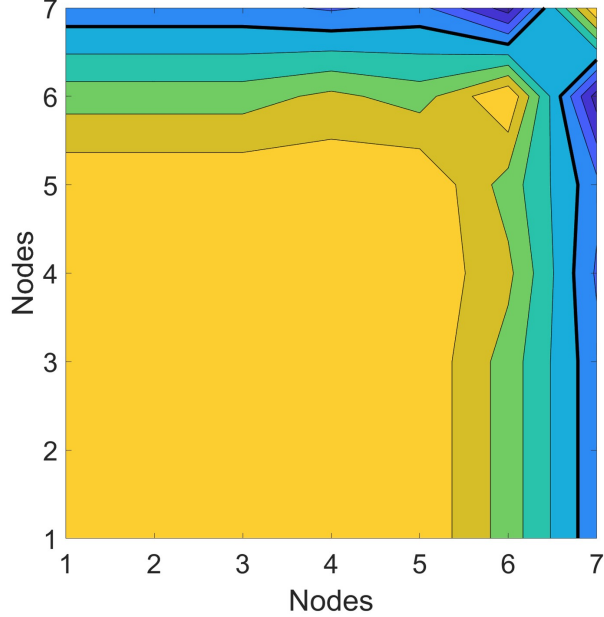


FIG. C.1: Contour plot of the signed communicability angle in the graph given in Fig. 4 of the main text. The contour line separating positive from negative values of the cosine of the communicability angle is marked with a thick black curve. This separation indicates that the communicability angle considers that vertices 1-6 forms a faction separated from vertex 7.

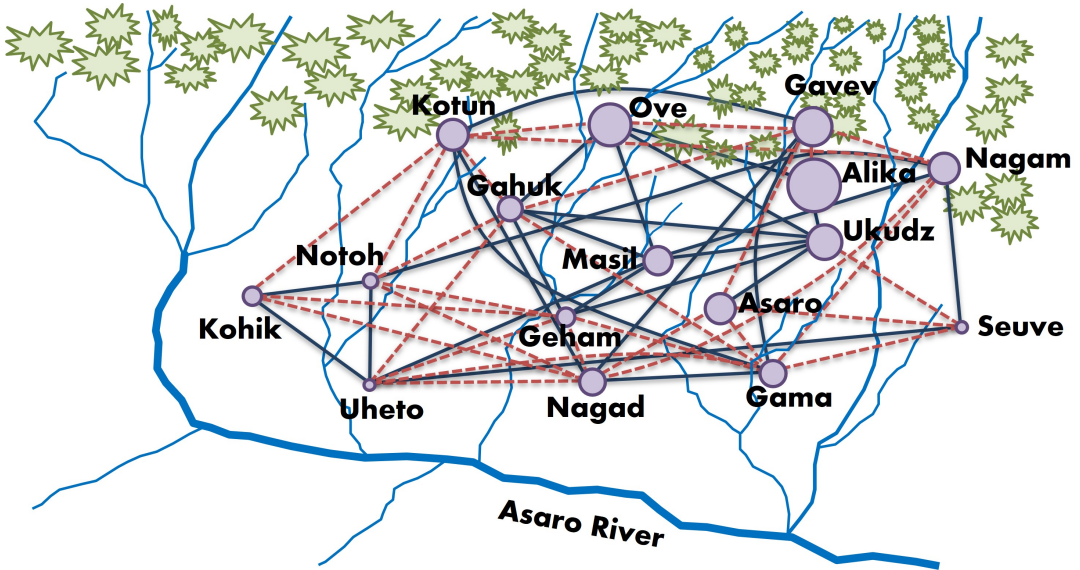


FIG. C.2: Sketch of the Gahuku-Gama network. The nodes are located in the geographical region that the corresponding tribe inhabits.

-
- [1] P. Tabaghi, J. Peng, O. Milenkovic, and I. Dokmanić, “Geometry of similarity comparisons,” *arXiv preprint arXiv:2006.09858*, 2020.
 - [2] T. Dittrich and G. Matz, “Signal processing on signed graphs: Fundamentals and potentials,” *IEEE Signal Processing Magazine*, vol. 37, pp. 86–98, Nov. 2020.
 - [3] T. Zaslavsky, “Signed graphs,” *Discrete Applied Mathematics*, vol. 4, pp. 47–74, Jan. 1982.

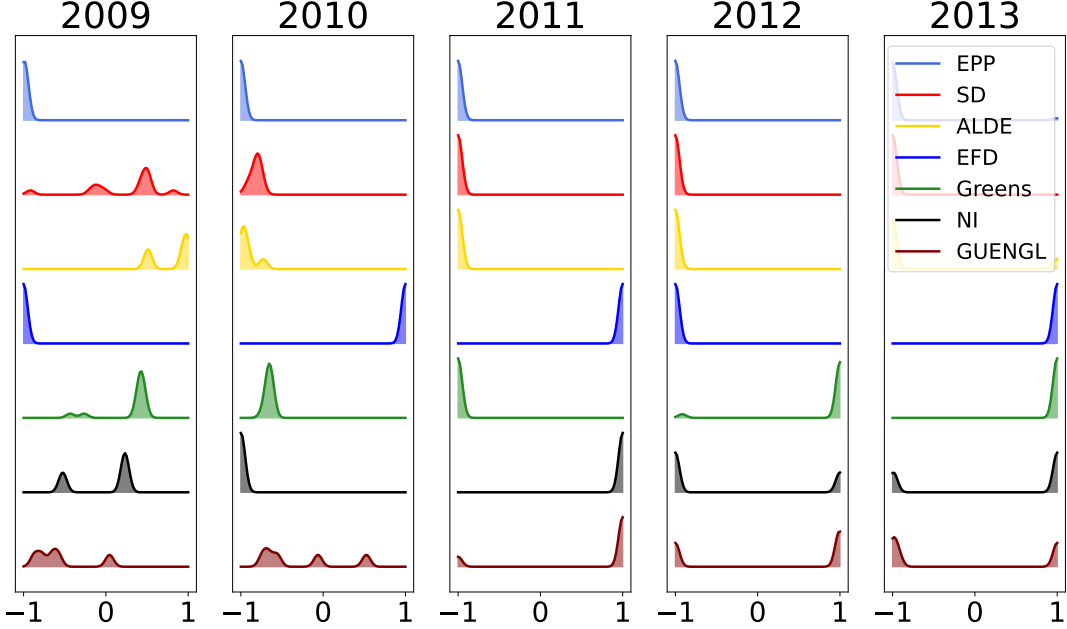


FIG. C.3: Latent polarization distribution of each political group for each network analyzed in the time range 2009-2014. The latent polarization is taken to be the first component of a PCA of the embedding shown in Fig. 9 of the main text. The pdfs were smoothed using kernel density estimation with Gaussian kernels and bandwidth $h = 0.05$.

- [4] X. Zheng, D. Zeng, and F.-Y. Wang, “Social balance in signed networks,” *Information Systems Frontiers*, vol. 17, pp. 1077–1095, Oct. 2015.
- [5] G. Iacono and C. Altafini, “Monotonicity, frustration, and ordered response: an analysis of the energy landscape of perturbed large-scale biological networks,” *BMC systems biology*, vol. 4, no. 1, pp. 1–14, 2010.
- [6] H. Saiz, J. Gómez-Gardeñes, P. Nuche, A. Girón, Y. Pueyo, and C. L. Alados, “Evidence of structural balance in spatial ecological networks,” *Ecography*, vol. 40, no. 6, pp. 733–741, 2017.
- [7] G. Facchetti, G. Iacono, and C. Altafini, “Computing global structural balance in large-scale signed social networks,” *Proceedings of the National Academy of Sciences*, vol. 108, no. 52, pp. 20953–20958, 2011.
- [8] M. Szell, R. Lambiotte, and S. Thurner, “Multirelational organization of large-scale social networks in an online world,” *Proceedings of the National Academy of Sciences*, vol. 107, pp. 13636–13641, Aug. 2010.
- [9] J. Leskovec, D. Huttenlocher, and J. Kleinberg, “Signed networks in social media,” in *Proceedings of the SIGCHI Conference on Human Factors in Computing Systems*, (Atlanta Georgia USA), pp. 1361–1370, ACM, Apr. 2010.
- [10] Z. P. Neal, “A sign of the times? Weak and strong polarization in the U.S. Congress, 1973–2016,” *Social Networks*, vol. 60, pp. 103–112, Jan. 2020.
- [11] F. Harary, “A structural analysis of the situation in the middle east in 1956,” *Journal of Conflict Resolution*, vol. 5, no. 2, pp. 167–178, 1961.
- [12] E. M. Hafner-Burton, M. Kahler, and A. H. Montgomery, “Network analysis for international relations,” *International organization*, vol. 63, no. 3, pp. 559–592, 2009.
- [13] F. Diaz-Diaz, P. Bartesaghi, and E. Estrada, “Network theory meets history. Local balance in global international relations,” *arXiv preprint arXiv:2303.03774*, 2023.
- [14] J. W. Baron, “Eigenvalue spectra and stability of directed complex networks,” *Physical Review E*, vol. 106, no. 6, p. 064302, 2022.
- [15] M. MacMahon and D. Garlaschelli, “Community detection for correlation matrices,” *Physical Review. X*, vol. 5, no. 2, 2015.
- [16] E. Ferreira, S. Orbe, J. Ascorbebeitia, B. Álvarez Pereira, and E. Estrada, “Loss of structural balance in stock markets,” *Scientific Reports*, vol. 11, no. 1, p. 12230, 2021.
- [17] P. Hage, “Graph theory as a structural model in cultural anthropology,” *Annual Review of Anthropology*, vol. 8, no. 1, pp. 115–136, 1979.
- [18] P. Hage and F. Harary, “Some genuine graph models in anthropology,” *Journal of graph theory*, vol. 10, no. 3, pp. 353–361, 1986.

- [19] D. R. White, V. Batagelj, and A. Mrvar, "Anthropology: Analyzing large kinship and marriage networks with Pgraph and Pajek," *Social Science Computer Review*, vol. 17, no. 3, pp. 245–274, 1999.
- [20] N. Arinik, R. Figueiredo, and V. Labatut, "Signed graph analysis for the interpretation of voting behavior," *arXiv preprint arXiv:1712.10157*, 2017.
- [21] N. Arinik, R. Figueiredo, and V. Labatut, "Multiple partitioning of multiplex signed networks: Application to european parliament votes," *Social Networks*, vol. 60, pp. 83–102, 2020.
- [22] Z. P. Neal, "A sign of the times? weak and strong polarization in the us congress, 1973–2016," *Social Networks*, vol. 60, pp. 103–112, 2020.
- [23] S. Talaga, M. Stella, T. J. Swanson, and A. S. Teixeira, "Polarization and multiscale structural balance in signed networks," *Communications Physics*, vol. 6, pp. 1–15, Dec. 2023.
- [24] B. Healy and A. Stein, "The balance of power in international history: theory and reality," *Journal of Conflict Resolution*, vol. 17, no. 1, pp. 33–61, 1973.
- [25] D. M. Kilgour, K. W. Hipel, and L. Fang, "The graph model for conflicts," *Automatica*, vol. 23, no. 1, pp. 41–55, 1987.
- [26] Z. Maoz, *Networks of nations: The evolution, structure, and impact of international networks, 1816–2001*, vol. 32. Cambridge University Press, 2010.
- [27] P. Doreian and A. Mrvar, "Structural balance and signed international relations," *Journal of Social Structure*, vol. 16, no. 1, pp. 1–49, 2015.
- [28] A. Kirkley, G. T. Cantwell, and M. E. J. Newman, "Balance in signed networks," *Physical Review E*, vol. 99, p. 012320, Jan. 2019.
- [29] A. Corradi, C. McMillan, and N. Dietrich, "A hostile reputation: A social network approach to interstate hostility," *Social Networks*, vol. 71, pp. 61–69, 2022.
- [30] F. Harary, "On the notion of balance of a signed graph.,," *Michigan Mathematical Journal*, vol. 2, no. 2, pp. 143–146, 1953.
- [31] F. Harary, "On local balance and N-balance in signed graphs.,," *Michigan Mathematical Journal*, vol. 3, no. 1, pp. 37–41, 1955.
- [32] D. Cartwright and F. Harary, "Structural balance: a generalization of Heider's theory.,," *Psychological review*, vol. 63, no. 5, p. 277, 1956.
- [33] S. Aref and Z. P. Neal, "Identifying hidden coalitions in the US House of Representatives by optimally partitioning signed networks based on generalized balance," *Scientific Reports*, vol. 11, p. 19939, Oct. 2021.
- [34] P. Guerra, W. M. Jr, C. Cardie, and R. Kleinberg, "A Measure of Polarization on Social Media Networks Based on Community Boundaries," *Proceedings of the International AAAI Conference on Web and Social Media*, vol. 7, no. 1, pp. 215–224, 2013.
- [35] M. Hohmann, K. Devriendt, and M. Coscia, "Quantifying ideological polarization on a network using generalized Euclidean distance," *Science Advances*, vol. 9, p. eabq2044, Mar. 2023.
- [36] J. Kunegis, "Applications of Structural Balance in Signed Social Networks," Feb. 2014.
- [37] X. Liu, Z. Ji, and T. Hou, "Graph partitions and the controllability of directed signed networks," *Science China Information Sciences*, vol. 62, p. 42202, Mar. 2019.
- [38] S. Talaga, M. Stella, T. J. Swanson, and A. S. Teixeira, "Polarization and multiscale structural balance in signed networks," Apr. 2023.
- [39] Y. Tian and R. Lambiotte, "Spreading and structural balance on signed networks," *SIAM Journal on Applied Dynamical Systems*, vol. 23, no. 1, pp. 50–80, 2024.
- [40] F. Heider, "Attitudes and Cognitive Organization," *The Journal of Psychology*, vol. 21, pp. 107–112, Jan. 1946.
- [41] Y. Hou, J. Li, and Y. Pan, "On the Laplacian eigenvalues of signed graphs," *Linear and Multilinear Algebra*, vol. 51, no. 1, pp. 21–30, 2003.
- [42] S. Spiro, "The Wiener index of signed graphs," *Applied Mathematics and Computation*, vol. 416, p. 126755, Mar. 2022.
- [43] S. K. Hameed, T. V. Shijin, P. Soorya, K. A. Germina, and T. Zaslavsky, "Signed distance in signed graphs," *Linear Algebra and its Applications*, vol. 608, pp. 236–247, Jan. 2021.
- [44] S. Fortunato and D. Hric, "Community detection in networks: A user guide," *Physics reports*, vol. 659, pp. 1–44, 2016.
- [45] M. A. Javed, M. S. Younis, S. Latif, J. Qadir, and A. Baig, "Community detection in networks: A multidisciplinary review," *Journal of Network and Computer Applications*, vol. 108, pp. 87–111, 2018.
- [46] P. Doreian and A. Mrvar, "A partitioning approach to structural balance," *Social Networks*, vol. 18, pp. 149–168, Apr. 1996.
- [47] A. Hassan, A. Abu-Jbara, and D. Radov, "Extracting Signed Social Networks from Text," in *Workshop Proceedings of TextGraphs-7: Graph-based Methods for Natural Language Processing* (I. Matveeva, A. Hassan, and G. Dias, eds.), (Jeju, Republic of Korea), pp. 6–14, Association for Computational Linguistics, July 2012.
- [48] V. A. Traag and J. Bruggeman, "Community detection in networks with positive and negative links," *Physical Review E*, vol. 80, p. 036115, Sept. 2009.
- [49] M. J. Brusco and P. Doreian, "Partitioning signed networks using relocation heuristics, tabu search, and variable neighborhood search," *Social Networks*, vol. 56, pp. 70–80, Jan. 2019.
- [50] M. Ehsani and R. Mansouri, "BridgeCut: A new algorithm for balanced partitioning of signed networks," preprint, In Review, Jan. 2023.
- [51] F. Bonchi, E. Galimberti, A. Gionis, B. Ordozgoiti, and G. Ruffo, "Discovering polarized communities in signed networks," in *Proceedings of the 28th ACM International Conference on Information and Knowledge Management*, CIKM '19, (New York, NY, USA), pp. 961–970, Association for Computing Machinery, Nov. 2019.
- [52] V. A. Traag, P. Doreian, and A. Mrvar, "Partitioning signed networks," Mar. 2018.

- [53] J. Kunegis, S. Schmidt, A. Lommatzsch, J. Lerner, E. W. De Luca, and S. Albayrak, "Spectral Analysis of Signed Graphs for Clustering, Prediction and Visualization," in *Proceedings of the 2010 SIAM International Conference on Data Mining (SDM)*, Proceedings, pp. 559–570, Society for Industrial and Applied Mathematics, Apr. 2010.
- [54] Q. Zheng and D. Skillicorn, "Spectral Embedding of Signed Networks," in *Proceedings of the 2015 SIAM International Conference on Data Mining*, pp. 55–63, Society for Industrial and Applied Mathematics, June 2015.
- [55] K.-Y. Chiang, J. J. Whang, and I. S. Dhillon, "Scalable clustering of signed networks using balance normalized cut," in *Proceedings of the 21st ACM International Conference on Information and Knowledge Management*, CIKM '12, (New York, NY, USA), pp. 615–624, Association for Computing Machinery, Oct. 2012.
- [56] A. Knyazev, "On spectral partitioning of signed graphs," in *2018 Proceedings of the Seventh SIAM Workshop on Combinatorial Scientific Computing*, pp. 11–22, SIAM, 2018.
- [57] M. Cucuringu, P. Davies, A. Glielmo, and H. Tyagi, "SPONGE: A generalized eigenproblem for clustering signed networks," in *Proceedings of the Twenty-Second International Conference on Artificial Intelligence and Statistics*, pp. 1088–1098, PMLR, Apr. 2019.
- [58] M. E. J. Newman and M. Girvan, "Finding and evaluating community structure in networks," *Physical Review E*, vol. 69, p. 026113, Feb. 2004.
- [59] Y. Li, J. Liu, and C. Liu, "A comparative analysis of evolutionary and memetic algorithms for community detection from signed social networks," *Soft Computing*, vol. 18, pp. 329–348, Feb. 2014.
- [60] S. Gómez, P. Jensen, and A. Arenas, "Analysis of community structure in networks of correlated data," *Physical Review E, Statistical, Nonlinear, and Soft Matter Physics*, vol. 80, p. 016114, July 2009.
- [61] A. Amelio and C. Pizzuti, "Community mining in signed networks: a multiobjective approach," in *Proceedings of the 2013 IEEE/ACM international conference on advances in social networks analysis and mining*, pp. 95–99, 2013.
- [62] W. Chen, L. V. S. Lakshmanan, and C. Castillo, *Information and Influence Propagation in Social Networks*. No. 4, 2013.
- [63] J. Q. Jiang, "Stochastic block model and exploratory analysis in signed networks," *Physical Review E*, vol. 91, no. 6, p. 062805, 2015.
- [64] T. P. Peixoto, "Nonparametric weighted stochastic block models," *Physical Review E*, vol. 97, no. 1, p. 012306, 2018.
- [65] Y. Chen, X.-l. Wang, and B. Yuan, "Overlapping community detection in signed networks," *arXiv preprint arXiv:1310.4023*, 2013.
- [66] B. Yang, W. Cheung, and J. Liu, "Community Mining from Signed Social Networks," *IEEE Transactions on Knowledge and Data Engineering*, vol. 19, pp. 1333–1348, Oct. 2007.
- [67] L.-Q. Kong and M.-L. Yang, "Improvement of clustering algorithm FEC for signed networks," *Journal of Computer Applications*, vol. 31, no. 5, pp. 1395–1399, 2011.
- [68] J. Wu, L. Zhang, Y. Li, and Y. Jiao, "Partition signed social networks via clustering dynamics," *Physica A: Statistical Mechanics and its Applications*, vol. 443, pp. 568–582, Feb. 2016.
- [69] S. A. Babul and R. Lambiotte, "SHEEP, a signed hamiltonian eigenvector embedding for proximity," *Communications Physics*, vol. 7, no. 1, p. 8, 2024.
- [70] A.-M. Kermarrec and A. Moin, "Energy models for drawing signed graphs," 2011.
- [71] J. Pougué-Biyong, A. Gupta, A. Haghghi, and A. El-Kishky, "Learning Stance Embeddings from Signed Social Graphs," in *Proceedings of the Sixteenth ACM International Conference on Web Search and Data Mining*, (Singapore Singapore), pp. 177–185, ACM, Feb. 2023.
- [72] K. Garimella, G. D. F. Morales, A. Gionis, and M. Mathioudakis, "Quantifying controversy on social media," *ACM Transactions on Social Computing*, vol. 1, pp. 3:1–3:27, Jan. 2018.
- [73] S. Martin-Gutierrez, J. C. Losada, and R. M. Benito, "Multipolar social systems: Measuring polarization beyond dichotomous contexts," *Chaos, Solitons & Fractals*, vol. 169, p. 113244, Apr. 2023.
- [74] R. Singh and B. Adhikari, "Measuring the balance of signed networks and its application to sign prediction," *Journal of Statistical Mechanics: Theory and Experiment*, vol. 2017, p. 063302, June 2017.
- [75] S.-H. Yang, A. J. Smola, B. Long, H. Zha, and Y. Chang, "Friend or frenemy? Predicting signed ties in social networks," in *Proceedings of the 35th International ACM SIGIR Conference on Research and Development in Information Retrieval*, SIGIR '12, (New York, NY, USA), pp. 555–564, Association for Computing Machinery, Aug. 2012.
- [76] M. Fiedler, "Algebraic connectivity of graphs," *Czechoslovak Mathematical Journal*, vol. 23, no. 2, pp. 298–305, 1973.
- [77] U. von Luxburg, "A tutorial on spectral clustering," *Statistics and Computing*, vol. 17, pp. 395–416, Dec. 2007.
- [78] D. L. Powers, "Graph partitioning by eigenvectors," *Linear Algebra and its Applications*, vol. 101, pp. 121–133, 1988.
- [79] Y. Liu, Z. Li, H. Xiong, X. Gao, and J. Wu, "Understanding of internal clustering validation measures," in *2010 IEEE international conference on data mining*, pp. 911–916, IEEE, 2010.
- [80] M. Pereda and E. Estrada, "Visualization and machine learning analysis of complex networks in hyperspherical space," *Pattern Recognition*, vol. 86, pp. 320–331, 2019.
- [81] S. Fortunato and M. Barthélémy, "Resolution limit in community detection," *Proceedings of the National Academy of Sciences*, vol. 104, pp. 36–41, Jan. 2007.
- [82] E. Estrada, "The many facets of the estrada indices of graphs and networks," *SeMA Journal*, vol. 79, no. 1, pp. 57–125, 2022.
- [83] E. Estrada and M. Benzi, "Walk-based measure of balance in signed networks: Detecting lack of balance in social networks," *Physical Review E*, vol. 90, no. 4, p. 042802, 2014.
- [84] J. Gower, "Properties of euclidean and non-euclidean distance matrices," *Linear Algebra and its Applications*, vol. 67, pp. 81–97, 1985.
- [85] N. Krislock and H. Wolkowicz, *Euclidean distance matrices and applications*. Springer, 2012.

- [86] E. Estrada, M. G. Sánchez-Lirola, and J. A. de la Peña, “Hyperspherical embedding of graphs and networks in communicability spaces,” *Discrete Applied Mathematics*, vol. 176, pp. 53–77, Oct. 2014.
- [87] K. E. Read, “Cultures of the central highlands, new guinea,” *Southwestern Journal of Anthropology*, vol. 10, no. 1, pp. 1–43, 1954.
- [88] A. Mead, “Review of the development of multidimensional scaling methods,” *Journal of the Royal Statistical Society: Series D (The Statistician)*, vol. 41, no. 1, pp. 27–39, 1992.
- [89] P. J. Rousseeuw, “Silhouettes: a graphical aid to the interpretation and validation of cluster analysis,” *Journal of computational and applied mathematics*, vol. 20, pp. 53–65, 1987.
- [90] J. H. Ward Jr, “Hierarchical grouping to optimize an objective function,” *Journal of the American statistical association*, vol. 58, no. 301, pp. 236–244, 1963.
- [91] F. Pedregosa, G. Varoquaux, A. Gramfort, V. Michel, B. Thirion, O. Grisel, M. Blondel, P. Prettenhofer, R. Weiss, V. Dubourg, J. Vanderplas, A. Passos, D. Cournapeau, M. Brucher, M. Perrot, and E. Duchesnay, “Scikit-learn: Machine learning in Python,” *Journal of Machine Learning Research*, vol. 12, pp. 2825–2830, 2011.
- [92] S. Rinke, *Latin America and the First World War*. Cambridge University Press, 2017.
- [93] N. Masuda, Z. M. Boyd, D. Garlaschelli, and P. J. Mucha, “Correlation networks: Interdisciplinary approaches beyond thresholding,” *arXiv preprint arXiv:2311.09536*, 2023.
- [94] J. Sherman, “Adjustment of an inverse matrix corresponding to changes in the elements of a given column or a given row of the original matrix,” *Annals of mathematical statistics*, vol. 20, no. 4, p. 621, 1949.